American Journal of Pathology, Vol. 128, No. 3, September 1987

Acute Injury and Regeneration of the Mesothelium in Response to Asbestos Fibers

PAMELA A. MOALLI, BA,
JANICE L. MACDONALD, BA,
LEE A. GOODGLICK, BS,
and AGNES B. KANE, MD, PhD

From the Department of Pathology and Laboratory Medicine, Brown University, Providence, Rhode Island

The mesothelium is a target of the toxic and carcinogenic effects of asbestos fibers. Fibers greater than 8 μ in length and less than 0.25 μ in diameter have been found to be highly tumorigenic in rodents, while shorter asbestos fibers or spherical mineral particles have not been shown to produce mesotheliomas. For investigation of early mesothelial reactions associated with the development of mesotheliomas, C57BL/6 mice were given intraperitoneal injections of 200 μg of short or long crocidolite asbestos fibers, toxic silica particles, or nontoxic titanium dioxide particles. At intervals between 3 hours and 21 days after a single injection, the mesothelial surface of the diaphragm was examined by stereomicroscopy, scanning electron microscopy, and autoradiography. Within 6 hours after injection of asbestos fibers, mesothelial cells in the lacunar regions of the diaphragm retracted opening stomata 10.7 $\pm$ 2.3 μ in diameter leading to the submesothelial lymphatic plexus. Short asbestos fibers (90.6% $\leq$ 2 μ in length), silica, or titanium dioxide particles ($\leq$ 5 μ in diameter) were cleared through these stomata without provoking an inflammatory reaction or mesothelial injury. In contrast, long asbestos fibers (60.3% $\geq$ 2 μ in length) were trapped at the lymphatic stomata in the lacunar regions on the peritoneal surface of the diaphragm. At these sites, an intense inflammatory reaction developed with accumulation of activated macrophages and a 5.5-fold increase in albumin recovered in the peritoneal lavage fluid after 3 days. As early as 12 hours after injection of long asbestos fibers, the adjacent mesothelial cells were unable to exclude trypan blue and lost their surface microvilli, developed blebs, and detached. Recovery of lactate dehydrogenase activity in the peritoneal lavage fluid was increased 5.8-fold after 3 days and returned to normal levels after 14 days. Regenerating mesothelial cells appeared at the periphery of asbestos fiber clusters 3 days after injection. Maximal incorporation of ^{3}H-thymidine by mesothelial cells occurred after 7 days, followed by partial restoration of the mesothelial lining after 14–21 days. As late as 6 months after a single injection of crocidolite asbestos fibers, clusters of fibers remained in the lacunar regions, partially covered by mesothelium but surrounded by macrophages and regenerating mesothelial cells. The anatomic distribution and size of lymphatic stomata on the peritoneal surface of the diaphragm account for the selective accumulation of long asbestos fibers in these regions. Activated macrophages at these sites may provoke leakage of reactive oxygen metabolites, resulting in mesothelial cell injury followed by regeneration. It is hypothesized that repeated episodes of injury and regeneration may promote the development of mesotheliomas. (Am J Pathol 1987, 128:426–445)

EXPOSURE to asbestos fibers is associated with the development of mesotheliomas, malignant tumors arising from the pleural or peritoneal lining.[1,2] Spherical mineral particles such as silica[3] or titanium dioxide[4] do not produce these tumors, although both asbestos fibers[5] and silica[6] cause pulmonary fibrosis. Mesotheliomas develop in experimental animals following inhalation[7] or direct intrapleural or intraperitoneal implantation of several types of mineral fibers, including different forms of asbestos and glass fibers.[8–10] On the basis of these experiments the Stanton hypothesis was formulated: fibers longer than 8 μ and thinner than 0.25 μ, regardless of their chemical composition, are responsible for mesotheliomas. More recently, other investigators have identified additional factors, including surface charge and ionic composition, which may also contribute to the development of these tumors.[11]

Supported by NIH Grants KO4 ES 00127, RO1 ES 03721, and RO1 ES 03189. Lee A. Goodglick was supported as a trainee by NIH Grant T32 GM 07601.

Accepted for publication April 21, 1987.

Address reprint requests to Dr. Agnes B. Kane, Division of Biology and Medicine, Brown University, Box G, Providence, RI 02912.

The mechanism leading to the development of mesotheliomas is unknown. Asbestos may act as a complete carcinogen or as a tumor promoter. Unlike most chemical carcinogens, asbestos fibers are not directly mutagenic in bacterial[12] or mammalian assay systems.[13,14] Asbestos fibers also do not damage cellular DNA,[15,16] although they are clastogenic.[17,18] Rat or human pleural mesothelial cells phagocytize asbestos fibers *in vitro*.[19,20] These fibers are highly toxic to cultured mesothelial cells, producing chromosomal aberrations and morphologic changes. Colonies of mesothelial cells with altered growth characteristics arise during exposure to asbestos fibers *in vitro*; however, these altered cells have not yet been shown to be tumorigenic.[21,22] It is also possible that asbestos acts as a tumor promoter. When applied to cultured hamster tracheal epithelial cells, asbestos fibers produce several metabolic alterations characteristic of tumor promoters.[23–25] In other *in vitro* assays, asbestos fibers do not appear to act as tumor promoters. For example, asbestos fibers do not enhance benzo(a)pyrene-induced transformation of rat pleural mesothelial cells[26] or inhibit metabolic cooperation in the V79 assay system.[27] These results raise the possibility that asbestos fibers may indirectly promote the development of mesotheliomas via their effects on phagocytes. In support of an indirect mechanism is the observation that asbestos fibers trigger the release of reactive oxygen metabolites from macrophages[28,29] and cultured tracheal epithelial cells.[30] Activated phagocytes have been shown previously to induce point mutations,[31] chromosomal damage,[32] and transformation of cocultured fibroblasts.[33] These experiments led to the hypothesis that asbestos fibers stimulate the local release of reactive oxygen species from phagocytes, thus creating a "prooxidant environment" favoring the development of tumors.[34]

It is not known whether asbestos fibers directly or indirectly cause mesothelial cell injury and altered growth regulation *in vivo*. Numerous investigations have confirmed that mesotheliomas develop 1–3 years after exposure of rodents to asbestos fibers; however, the initial reaction of the mesothelial lining to asbestos and other mineral particles has not been described.[35,36] On the basis of the Stanton hypothesis, we predicted that only long asbestos fibers will interact with and damage the mesothelial lining. We tested this prediction by comparing the morphologic reactions of the mesothelium to intraperitoneal injection of short or long asbestos fibers and spherical mineral particles which are not carcinogenic. Four reactions were observed: 1) the anatomic location of these three types of minerals, 2) the intensity of the inflammatory response, 3) the extent of mesothelial injury, and 4) mesothelial regeneration. The anatomic location of asbestos fibers was identified morphologically and confirmed by fiber counts following tissue digestion. The inflammatory response was described morphologically and quantitated by recovery of albumin in peritoneal lavage fluid. Cell injury was described morphologically and confirmed by a dye exclusion assay and release of lactate dehydrogenase activity into the peritoneal lavage fluid. Mesothelial cell regeneration was observed morphologically and proliferation was documented by autoradiography after injection of ^{3}H-thymidine.

Materials and Methods

Preparation of Mineral Particle Stocks

Crocidolite asbestos fibers, crystalline silica particles (quartz), and titanium dioxide particles (rutile) were obtained from stocks originally prepared and characterized by the Union Internationale Contre Le Cancer (Timbrell, 1971/72).[37] The asbestos fibers and titanium dioxide particles were purchased from Duke Scientific Corporation (Palo Alto, Calif); silica particles ($\leq 5\ \mu$ in diameter) were a gift from Dr. R. E. G. Rendall, National Centre for Occupational Health, P.O. Box 4788, Johannesburg 2000, Republic of South Africa. The native preparation of crocidolite asbestos fibers will be referred to as "mixed fibers." This preparation was separated into "long" and "short" fibers by differential centrifugation and filtration, modified from the procedure of Brody et al (1983)[38] as follows. Native crocidolite asbestos fibers (0.5–1.0 g) were suspended in 10 ml of deionized water and centrifuged at 1200 rpm for 10 minutes in an IEC Centra-7R centrifuge. The upper layer contained the starting material for short fibers; the pellet was the starting material for long fibers. The pellet was resuspended in deionized water and centrifuged as described above; this sequence was repeated nine times. The short fibers were placed in a 500-ml sterile Nalgene filter apparatus (Fisher Scientific Company, Medford, Mass), collected by vacuum filtration, rinsed with absolute ethanol, and air-dried under a laminar flow hood equipped with Hepa filters. The fibers were gently scraped off the filter and placed in a preweighed glass vial. The pellets containing long fibers were resuspended in 10 ml of deionized water and centrifuged at 1,000 rpm for 10 minutes. The pellet was resuspended in 10 ml of deionized water, then centrifuged at 500 rpm for 5 minutes. The pellet was then resuspended in 10 ml of deionized water and filtered through 100-μ nylon mesh (TETKO, Inc., Elmsford, NY) in a Nalgene 250 ml filter apparatus (Fisher Scientific Company). The fibers were collected by vacuum filtration, rinsed with absolute eth-

anol, and air-dried. The fibers were collected from the top of the nylon mesh and placed in a preweighed glass vial.

Stock suspensions of all mineral particles and fiber preparations were prepared in Dulbecco's phosphate-buffered saline, pH 7.4 (PBS, Grand Island Biological Co., Grand Island, NY) at a concentration of 200 μg/ml, autoclaved, and sonicated in a water bath for 20 minutes prior to intraperitoneal injection. Where indicated, mice also received an injection of 1 ml of PBS alone or 1.5 ml of thioglycollate broth (4% wt/vol; Difco Laboratories, Detroit, Mich), an agent which produces nonspecific activation of mouse peritoneal macrophages.[39]

Dimensions of Crocidolite Asbestos Fiber Preparations

The stock suspensions of mixed, long, or short asbestos fibers were sonicated for 20 minutes. A 75-μl aliquot was taken from each suspension and diluted with 925 μl of deionized water which had been filtered through a Millipore Millex-GV 0.22-μ filter unit (Millipore Corp., Bedford, Mass). A 5-μl aliquot from the mixed and long fiber preparations was placed on formvar-coated copper grids (100 windows/grid; Polaron Corp., Hatfield, Pa). The short fibers were diluted 1:5 with filtered, deionized water and a 5-μl aliquot placed on formvar-coated grids. The samples on grids were placed in a bell jar under vacuum for 90 minutes, then placed in a warming oven at 60 C overnight. Fibers were viewed in a Philips 410 transmission electron microscope. The exact magnification was calculated by using a calibration grating replica with 1200 lines/mm (Ernest F. Fullam, Inc., Schenectady, NY). Photographs of at least 20 windows per grid were taken at magnifications of 550.9× and 1597.5×. The total number of fibers per milligram was calculated at 550.9× magnification. Fiber lengths and fiber diameters were measured at magnifications of 550.9× and 1597.5×, respectively. Only fibers with a length to diameter ratio ≥ 3:1 were counted. No clumps of fibers were seen in these preparations. In agreement with the previous data obtained by Monchaux et al,[11] the native mixed fiber preparation of crocidolite asbestos contained 2.93×10^9 fibers/mg. There were 1.22×10^9 fibers/mg in the long fiber preparation, 4.64×10^9 fibers/mg in the short fiber preparation, 9.31×10^8 silica particles/mg, and 3.49×10^9 titanium dioxide particles/mg. The fiber dimensions are shown in Tables 1 and 2.

Intraperitoneal Injection of Mineral Particles

Male C57BL/6 mice were obtained from Charles River Laboratories (North Wilmington, Mass) at 2 months of age and given intraperitoneal injections of 200 μg/ml of crocidolite asbestos, silica, titanium dioxide, 1.5 ml of thioglycollate broth, or 1 ml of phosphate-buffered saline (PBS). The mice were kept in filter-top plastic cages and maintained as described previously.[40] The animals were sacrificed with an overdose of ether at the following times after injection: 3, 6, 12, or 24 hours; 3, 7, 14, 21 or 35 days; and 6 months. For each experiment, 2–6 mice were examined.

Table 1—Lengths of Crocidolite Asbestos Fiber Preparations

Length (μ)	% Fibers in size range		
	Mixed	Long	Short
0.1- 0.5	18.7	6.4	44.8
0.6- 1.0	27.6	11.1	29.6
1.1- 2.0	30.1	22.1	16.2
2.1- 5.0	15.1	32.9	8.3
5.1-10.0	4.4	15.1	1.1
10.1-15.0	0.9	5.7	0
15.1-20.0	1.5	2.3	0
20.1-25.0	0.4	1.0	0
25.1-30.0	0	0.7	0
30.1-35.0	0	0.3	0
0.0 ≥ 35.1	1.3	2.3	0

Native crocidolite asbestos fibers ("mixed") were fractionated into "long" and "short" fibers by a series of centrifugation and filtration steps. Aliquots of these preparations were mounted on formvar-coated grids and viewed in a Philips 410 transmission electron microscope. The number of fibers in each size range was counted as described in Materials and Methods.

Collection of Blood and Peritoneal Lavage Fluid

The mice were narcotized with CO_2 and 0.5 ml of blood was removed by cardiac puncture. After sacrifice, 8 ml of sterile PBS was injected intraperitoneally by means of a 22-gauge needle and the syringe gently depressed and withdrawn 5 times. Then 6 ml of this

Table 2—Diameters of Crocidolite Asbestos Fiber Preparations

Diameter (μ)	% Fibers in size range		
	Mixed	Long	Short
0.03-0.10	12.2	20.3	27.3
0.11-0.20	41.5	21.6	60.7
0.21-0.30	15.4	12.8	8.7
0.31-0.40	12.2	13.2	2.7
0.41-0.50	6.5	11.9	0.5
0.51-0.60	4.1	4.4	0
0.61-0.70	4.1	5.3	0
0.71-0.80	1.6	4.0	0
0.81-0.90	0	2.6	0
0.91-1.00	0	0.4	0
1.01-1.50	0.8	1.8	0
1.51-2.00	0.8	0.9	0
2.01-2.50	0.8	0.9	0
2.51-3.00	0	0	0

See legend to Figure 1.

fluid was withdrawn with a syringe. The cells were removed by centrifugation at 1500 rpm for 5 minutes in an IEC Centra-7R centrifuge at 4 C. The serum and peritoneal lavage fluids were used for biochemical analyses of albumin content and lactate dehydrogenase activity as described subsequently.

Fixation and Dissection of the Diaphragm

The anterior abdominal wall was cleaned with 95% ethanol, and the fur removed. The mesothelium was fixed *in situ* by injecting 10 ml of 2% paraformaldehyde and 2.5% glutaraldehyde in 0.1 M sodium cacodylate buffer, pH 7.4, at 4 C.[41] The mice were kept on ice for 20 minutes before further dissection. The skin was removed from the abdomen up to the level of the costal margins. The peritoneum was exposed through a midventral incision; lateral incisions were made extending to the vertebral column. The diaphragm was exposed by hyperextension of the vertebral column. The falciform ligament, esophagus, posterior vena cava, abdominal aorta, vertebral column, and psoas muscles were severed just caudal to the diaphragm freeing the thorax and head from the remainder of the body. The diaphragm, still attached to the rib cage, was rinsed in cold cacodylate buffer. The diaphragm was then cut around its perimeter, freed from its cardiac attachment, and rinsed three times in cacodylate buffer. The diaphragms were allowed to fix in the above fixative at 4 C overnight.

Recovery of Asbestos Fibers From Tissue Digests

Mice were injected intraperitoneally with 200 μg of mixed, short, or long preparations of crocidolite asbestos fibers. After 3 days, the mice were sacrificed and the diaphragm dissected as described subsequently. The falciform ligament and attached lymphatics were removed. The cleaned diaphragm was digested in 3 ml of bleach (5.25% sodium hypochlorite) for 5 hours at room temperature according to the procedure described by Churg and Warnock (1980)[42] with the following modifications. In order to minimize fiber clumping, 10 μl of 1% Tween-80 detergent (vol/vol; Sigma Chemical Co., St. Louis, Mo) was added. Under vacuum, 500 μl of this suspension was filtered through a Nucleopore membrane (13 mm in diameter; 0.1-μ pore size; VWR Scientific, Inc., Boston, Mass). The filter was rinsed with 1 ml of absolute ethanol, then for 30 minutes with 2 ml of 50% hydrogen peroxide (Fisher Scientific Co.), and finally with 5 ml of absolute ethanol. The filter was gold-coated with an ISI-PS-2 Sputter-Coater (Polaron, Hatfield, Pa) and viewed in an AMR 1000 scanning electron microscope at 20 kv at 500× magnification. At least 26 randomly selected fields were photographed for subsequent counting of fibers.

Examination by Stereomicroscopy

The fixed diaphragms were examined and photographed under a Nikon SMZ-10 dissecting stereophotomicroscope. Photographs of the entire diaphragm were taken with a 2× lens and used for gross orientation of fiber clusters. At 80× magnification, cuboidal mesothelial cells in the lacunar regions of the diaphragm were visible; longer asbestos fibers could also be seen at this magnification. Drawings of fiber clusters using the vascular bed as landmarks were made to assist in locating lesions to be studied by light microscopy, scanning electron microscopy, and autoradiography.

Examination by Light Microscopy

Lesions were dissected from the diaphragm under the stereomicroscope by means of a razor blade. These tissue samples were either embedded in paraffin or postfixed, dehydrated, and embedded in Spurr's resin as described previously.[40] Paraffin-embedded sections were cut at 6 μ and examined unstained with a phase-contrast microscope or stained with hematoxylin and eosin (H&E). Plastic-embedded sections were cut at 0.5 μ and stained with Giemsa solution (American Scientific Products, Medford, Mass), then briefly de-stained in ethanol. The stained sections were examined and photographed with a Zeiss Axioplan photomicroscope.

Examination by Scanning Electron Microscopy

The entire diaphragm or selected areas identified under the dissecting stereomicroscope were processed for examination by scanning electron microscopy as outlined by Harrison et al (1982).[43] Briefly, the fixed specimens were rinsed for 15 minutes in 0.1 M sodium cacodylate buffer pH 7.2, postfixed in 2% (wt/vol) osmium (Electron Microscopy Sciences, Fort Washington, Pa) in 0.2 M sodium cacodylate for 1–2 hours at room temperature, and rinsed in deionized water. The specimen was placed for 20 minutes in a 1% (wt/vol) solution of thiocarbohydrazide (TCH; Electron Microscopy Sciences) which had been freshly prepared from a filtered, saturated solution, then rinsed again in deionized water. The postfixation, rinsing, and TCH steps were repeated, followed by a final fixation step in osmium. The specimens were rinsed again in deionized water and dehydrated

for 15 minutes in 2,2'-dimethoxypropane (freshly acidified by adding 6 drops of concentrated HCl per 100 ml; Polysciences, Inc., Warrington, Pa). The specimens were dried in a Bomar 900 critical point dryer (Bomar, Spokane, Wash) with liquid CO_2 and mounted on stainless steel stubs. The peritoneal surface of the diaphragm was examined in an AMR 1000 scanning electron microscope operating at 20 kv at 200–2000× magnification.

Trypan Blue Assay

Mice were sacrificed and prepared for dissection of the diaphragm as described above except for omission of fixation *in situ*. The peritoneal surface of the diaphragm was exposed. While still attached to the rib cage and the falciform ligament, the diaphragm was submerged in PBS at 4 C on ice. The peritoneal surface was then suspended in a 0.13% trypan blue solution (Flow Laboratories, Inc., Rockville, Md) for 5 minutes at 4 C on ice. The diaphragm was then rinsed three times in PBS at 4 C on ice for 15 minutes and fixed in 2.5% glutaraldehyde in PBS for 20 minutes at 4 C. The diaphragm was dissected away from the rib cage and examined immediately under the dissecting stereomicroscope. Diaphragms from uninjected mice did not stain with trypan blue under these conditions.[44,45] Surface imprints of the superficial mesothelial layer were prepared by pressing the air-dried diaphragm against a glass coverslip coated with poly-L-lysine (Sigma; 0.1% wt/vol in deionized water) and mounting in Aquamount (Lerner Lab., New Haven, Conn) as described previously by Whitaker et al (1980).[46]

Autoradiography

One hour before sacrifice, mice were given an intraperitoneal injection of [^{3}H-methyl]-thymidine (5.0 μCi/g body weight; s.a. 6.7 Ci/mmol; New England Nuclear Corp., Boston, Mass). The diaphragm was removed as described earlier and fixed in 2.5% glutaraldehyde in PBS at 4 C overnight. The intact diaphragm was rinsed several hours in deionized water and dipped in NTB-2 emulsion (diluted 1 : 1 [vol/vol] in deionized water; Eastman Kodak Co., Rochester, NY) for 2 minutes in the dark. The specimens were exposed for 1 week at 4 C in the dark, developed in D-19 (Eastman Kodak Co.) and fixed in 25% (wt/vol) sodium thiosulfate (Eastman Kodak Co.). Residual emulsion was removed by several rinses in deionized water.[46,47]

The peritoneal surface of the diaphragm was examined under the dissecting stereomicroscope. Labelled nuclei were easily visualized at 70× magnification. Twenty areas in the muscular region of the diaphragm were selected randomly, and the number of labeled nuclei per square centimeter in each of these areas was counted at 70× magnification.

Biochemical Analyses of Peritoneal Lavage Fluid

The total amount of albumin recovered in the peritoneal lavage fluid was used as an index of increased vascular permeability which accompanies the inflammatory reaction to mineral particles.[48] Albumin content was determined by measuring the absorbance at 630 nm of the complex formed with bromcresol green. Bovine serum albumin (BSA) was used to establish a standard concentration curve.[49]

Recovery of lactate dehydrogenase (LDH) activity in the peritoneal lavage fluid was used as an index of damage to the peritoneal lining produced by injection of toxic mineral particles.[48] A 2-ml aliquot of peritoneal lavage fluid was concentrated in a BSA-pretreated Centricon 10 microconcentration unit (Amicon Corp., Danvers, Mass). The concentrate was brought up to 400 μl with 0.85% NaCl; 100 μl was used to measure the extent of conversion of pyruvic acid to lactic acid by LDH. The disappearance of pyruvic acid was determined colorimetrically at 428 nm by the formation of hydrazone from 2,4-dinitrophenylhydrazine as described by Cabaud and Wroblewski (1958).[50] Total LDH activity in lavage fluid was expressed in Berger–Broida units (1 unit of LDH activity reduces 4.8×10^{-4} μmol pyruvate/min). All assays were run at room temperature; reagents were obtained from Sigma Chemical Co.

Statistical Analyses

The means ± standard errors calculated from triplicate samples from control and experimental groups were tested for statistical significance by means of the Student *t* test.

Results

Localization of Asbestos Fibers

The anatomic distribution of asbestos fibers after a single intraperitoneal injection of 200 μg of native crocidolite asbestos was mapped under a dissecting stereomicroscope. Within 3 hours after injection, small clusters appeared on the peritoneal surface of the diaphragm concentrated at the musculotendinous junction and extending outward on the muscular region. After 24 hours, 8–30 fiber clusters were observed; they ranged in size from 14×29 μ up to 57 ×

100 μ. When examined at higher magnifications as shown in Figure 1, the fiber clusters were irregular in outline and adjacent to blood vessels. Occasional isolated long fibers were found lying between fiber clusters. Fibers continued to accumulate at these locations during the first 3 days after injection. Fewer fiber clusters were found at the following sites: the falciform ligament (0–4) and the intestinal mesenteries and omentum (0–3). This distribution did not change throughout 6 months after the initial injection.

The anatomic distribution of asbestos fibers parallels the major lymphatic drainage sites in the parietal peritoneum.[51,52] The openings or stomata of lymphatics at the peritoneal surface of the diaphragm are found between discrete rows of dome-shaped mesothelial cells radiating away from the musculotendinous junction; these areas are called lacunar regions.[53] These stomata lead to a submesothelial plexus of lymphatics which drain to collecting vessels in the muscular layer of the diaphragm.[54] Similar regions of lymphatic stomata are found in the omentum and mesenteries, especially around Kampmeier's foci or milky spots. Similar structures are found in the pleural cavity, especially on the pleural surface of the diaphragm, in the dorsal caudal area of the mediastinum, and in the infracostal regions.[52] The diaphragmatic stomata are the major route for clearance of particulates from the peritoneal cavity[41,55,56] due to negative pressure created by movement of the diaphragm during respiration.

We studied the response of the diaphragmatic lymphatic stomata to intraperitoneal injection of asbestos fibers using scanning electron microscopy. The morphologic appearance of the mesothelium in untreated or PBS-treated mice is shown in Figure 2. A row of dome-shaped mesothelial cells with a few adherent mononuclear cells extends across the muscular region of the diaphragm. The adjacent mesothelium is composed of flat, tightly adhering cells covered by numerous long, thin microvilli. After only 6 hours following injection of asbestos fibers, these dome-shaped cells in the lacunar regions retracted. The stomata between the cells are easily recognized in Figure 3. These stomata were measured 6–12 hours after injection of native crocidolite asbestos fibers and were found to be $10.7 \pm 2.3\ \mu$ (mean $\pm$ SD) in diameter. In untreated mice or after injection with saline, the stomata range from 0.5 to 3 μ in diameter.

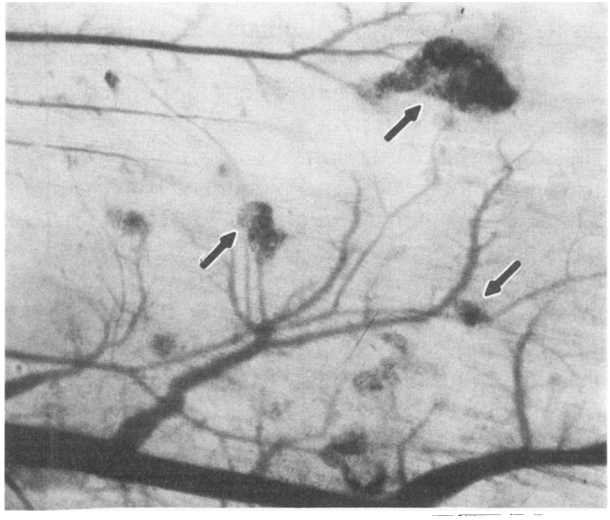

Figure 1—Light micrograph of a mouse diaphragm removed 24 hours after intraperitoneal injection of 200 μg of native (mixed lengths) crocidolite asbestos fibers as seen under a dissecting stereomicroscope. The *arrows* indicate clusters of fibers. (×100)

On the basis of these measurements and the anatomic distribution of asbestos fiber clusters in the lacunar regions on the diaphragm, we predicted that fibers less than the diameter of the lymphatic stomata would be cleared, while longer fibers would be trapped at the mesothelial surface in the lacunar regions. In order to test this prediction, native crocidolite asbestos fibers were fractionated into "short" and "long" fiber preparations as described in Materials and Methods. The dimensions of these fiber preparations are summarized in Tables 1 and 2: 90.6% of the short fibers are $\leq 2\ \mu$ long, and 60.3% of the long fibers are $\geq 2\ \mu$ long; 96.7% of the short fibers are $\leq 0.30\ \mu$ in diameter, and 54.7% of the long fibers are $\leq 0.30\ \mu$ in diameter. Mice were given intraperitoneal injections of 200 μg each of these fiber preparations. The anatomic distribution of these fibers on the diaphragm was determined by tissue digestion and fiber counting, stereomicroscopy, and scanning electron microscopy.

The number of short, mixed, or long preparations of asbestos fibers on the diaphragm was determined 3 days after injection following tissue digestion in bleach as described in Materials and Methods. After injection of mixed lengths of asbestos fibers 1.8×10^6 fibers were recovered from the diaphragm, and 9.6×10^5 fibers were recovered after injection of long asbestos fibers. In contrast, only 3.0×10^3 fibers were recovered after injection of short asbestos fibers. Examination of intact diaphragms by means of a dissecting stereomicroscope revealed clusters of fibers similar to those shown in Figure 1 after injection of either mixed or long fibers. No fiber clusters were found after injection of short fibers. Similar observations were made after injections of spherical silica or titanium dioxide particles ($\leq 5\ \mu$ in diameter). No aggregates of mineral particles were seen on the peritoneal surface of the diaphragm under either the

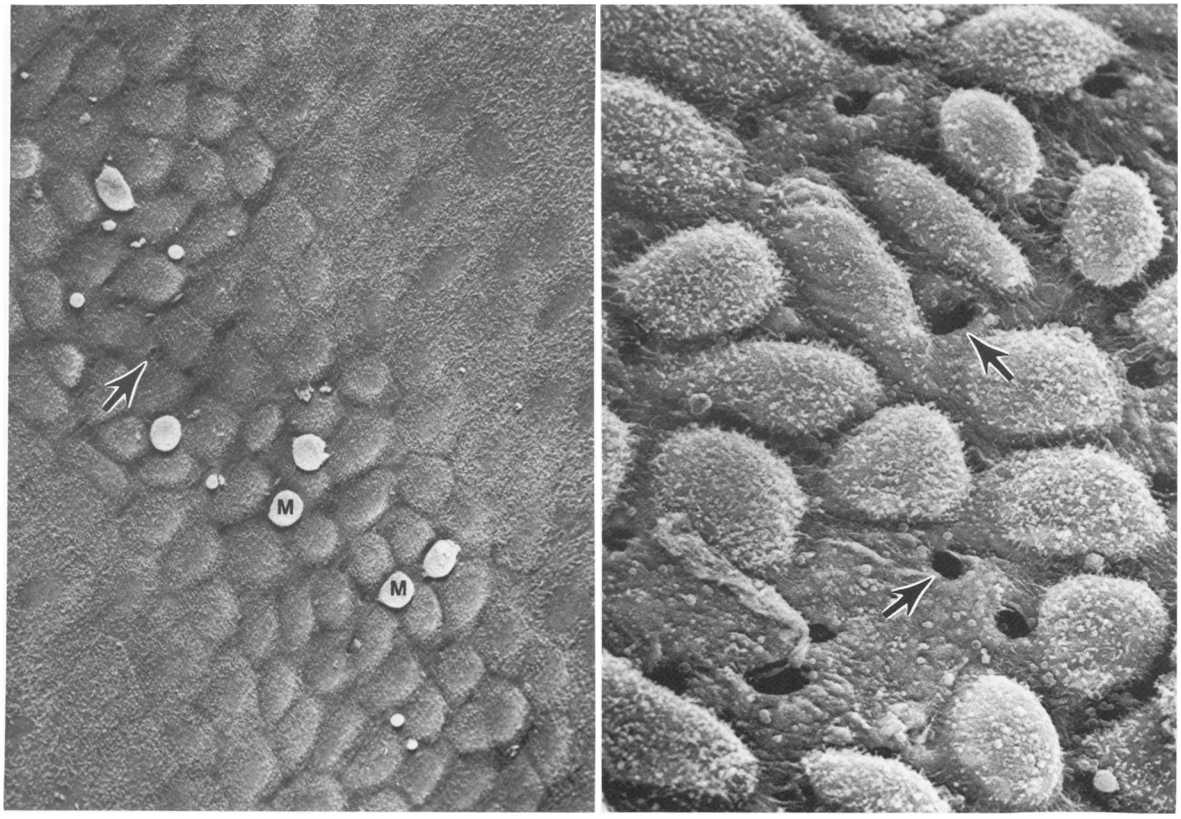

Figure 2—Scanning electron micrograph of the lacunar region of a diaphragm removed from an uninjected mouse. A row of cuboidal mesothelial cells extends diagonally across the photograph. A few mononuclear cells (*M*) are adherent to this surface. *Arrows* indicate occasional holes or stomata between the cuboidal cells. The adjacent mesothelial cells are flat and covered with fine microvilli. The intercellular junctions between these flat cells are tight with no stomata. (×580) **Figure 3**—Scanning electron micrograph of the lacunar region of a diaphragm removed 6 hours after injection of 200 μg of native (mixed lengths) crocidolite asbestos fibers. The cuboidal mesothelial cells have separated revealing numerous stomata indicated by arrows. (×1300)

dissecting stereomicroscope or the scanning electron microscope.

Clusters of mixed or long asbestos fibers were studied in more detail by light microscopy and scanning electron microscopy. A cross-section through a mixed fiber cluster embedded in plastic is shown in the light micrograph in Figure 4. The inset photographed under darkfield illumination shows numerous fibers, which appear white. The fibers are intermingled in and between inflammatory cells in this lesion. As shown in brightfield illumination, the fiber cluster is loosely adherent to the mesothelial surface above a dilated lymphatic channel in the submesothelial layer. The appearance of a similar fiber cluster by scanning electron microscopy is shown in Figure 5. At low magnification, no free fibers are evident; the clusters are completely covered by inflammatory cells. The extent of this inflammatory response will be described next.

Asbestos Fibers Elicit an Inflammatory Response

The earliest response to injection of mixed or long asbestos fibers is focal hemorrhage on the peritoneal surface of the diaphragm. As shown in Figure 6, fibrin, red blood cells, and platelets covered the mesothelium in lacunar regions 3–6 hours after injection of mixed asbestos fibers. This early hemorrhage was rapidly replaced by neutrophils and macrophages after 6–12 hours (Figure 5). After 3 days, macrophages were the most numerous cells in the fiber clusters, as shown in Figure 7. At this time, the macrophages had ruffled surfaces with prominent pseudopodia.[57] Many of these cells were distorted by the presence of long, thin fibers. All fibers visualized by scanning electron microscopy appeared to be covered by cellular membranes at these early time points. The maximal extent of this inflammatory reaction was found 3 days after injection. At this time, the

entire surface of the diaphragm was almost completely obscured by inflammatory cells. Many multinucleated giant cells were present. Between 14 and 21 days after injection of mixed or long asbestos fibers, the elevated lesions containing fiber clusters were still visible; however, only occasional macrophages were found on their surfaces.

The severity of this inflammatory response was monitored by recovery of albumin in the peritoneal lavage fluid measured as described in Materials and Methods. As shown by the open circles in Figure 8, increased levels of albumin were recovered after 3 hours and between 1 and 3 days after injection of long asbestos fibers. The early peak most likely reflects localized vascular damage, because fibrin and red blood cells were observed on the surface of the diaphragm at this time (Figure 6). The later peak reflects either increased vascular permeability accompanying the inflammatory response or reduced clearance of albumin from the peritoneum. It is unlikely that hemorrhage was responsible for increased albumin recovered in the peritoneal lavage fluid after 3 days, because only 3×10^3 red blood cells were recovered in the lavage fluid. This corresponds to 0.3 μl of whole blood, which would contribute only 9.9 μg of albumin. After 7 days, the amount of albumin recovered in the peritoneal lavage fluid declined. This time course parallels the severity of the inflammatory reaction observed by scanning electron microscopy.

The inflammatory response to injection of short asbestos fibers was also followed. As shown by the open triangles in Figure 8, there was only a small increase in the albumin recovered in the peritoneal lavage fluid 1–3 days after injection of 200 μg of short asbestos fibers. At these times, there also was little inflammatory reaction seen on the peritoneal surface of the diaphragm by scanning electron microscopy.

The inflammatory responses to intraperitoneal injection of a soluble irritant, thioglycollate broth, or the spherical mineral particles silica and titanium dioxide were compared. As shown by albumin recovery in the peritoneal lavage fluid after 3 days (Table 3), injection of thioglycollate or short asbestos fibers produced a small increase in albumin recovery ($P < 0.01$), whereas injection of titanium dioxide or silica particles did not significantly increase albumin recovery. This pattern was confirmed by examination of the diaphragm by scanning electron microscopy: little inflammatory reaction was observed at any time (1–21 days) after injection of these irritants.

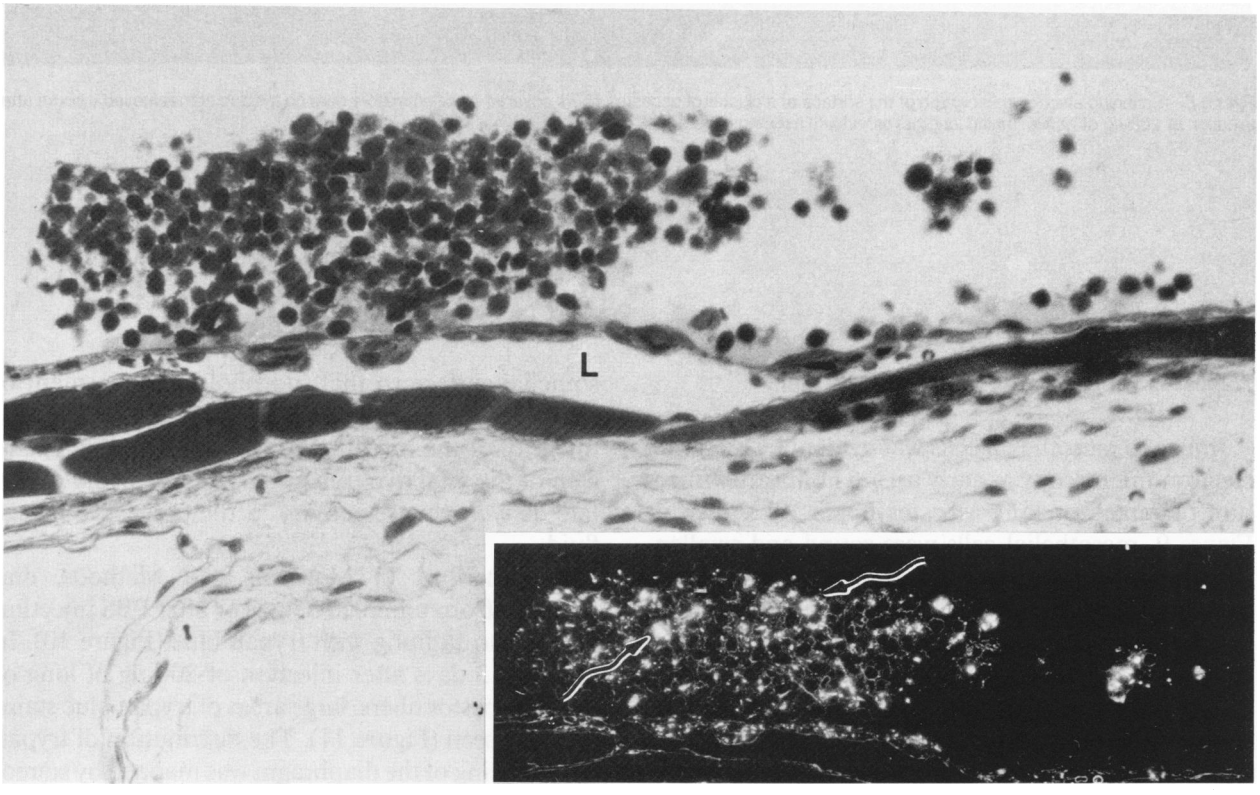

Figure 4—Light micrograph showing a cluster of asbestos fibers in cross-section at the musculotendinous junction of a diaphragm removed 12 hours after injection of 200 μg of native (mixed lengths) of asbestos fibers. With brightfield illumination, only inflammatory cells are easily identified. The inset by darkfield illumination shows numerous white fibers (*arrows*) within this group of inflammatory cells. This fiber cluster is located directly over a lymphatic channel (*L*) between the surface mesothelium and the underlying skeletal muscle. (×1700; **inset**, ×750)

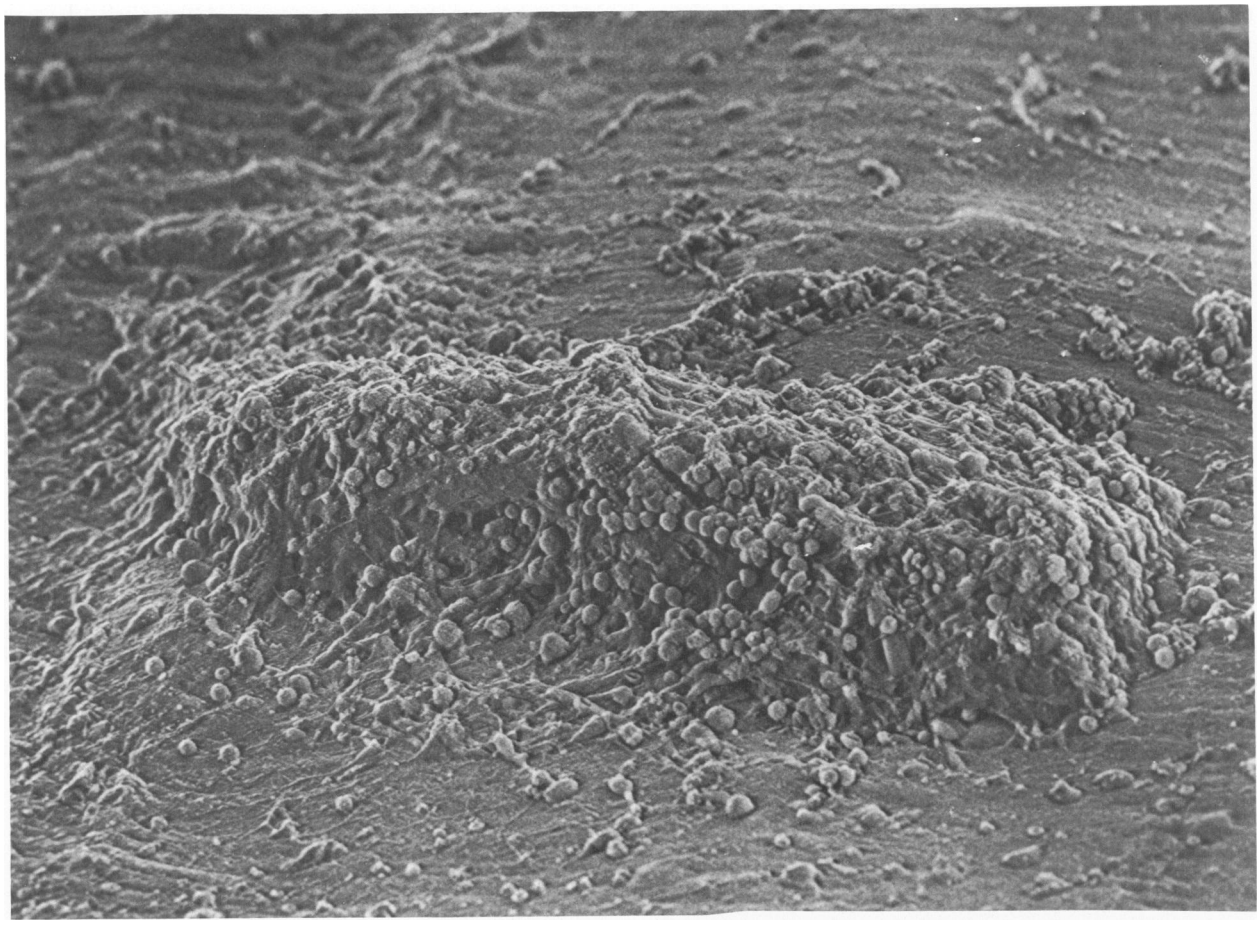

Figure 5—Scanning electron micrograph of the surface of a cluster of asbestos fibers covered by inflammatory cells on a diaphragm removed 6 hours after injection of 200 μg of native (mixed lengths) crocidolite asbestos fibers. (×320)

Asbestos Fibers Cause Mesothelial Injury

Injury to mesothelial cells was evident by scanning electron microscopy as early as 3–6 hours after injection of mixed or long asbestos fibers. As shown in Figure 9, mesothelial cells were round and swollen, with loss of surface microvilli. There was loss of intercellular junctions and formation of numerous surface blebs. Focal areas of cell detachment were seen, revealing the submesothelial connective tissue network. Dead cells (see lower corner of Figure 9) were shrunken and irregular and easily penetrated by the electron beam. After 12 hours, areas of injured and detached mesothelial cells were widespread on the surface of the diaphragm. At later times, the progressive infiltrate of inflammatory cells obscured the mesothelial surface so that morphologic assessment of the extent of injury was impossible. Therefore, the integrity of the mesothelium was assessed by exclusion of the vital dye trypan blue and recovery of lactate dehydrogenase activity in the peritoneal lavage fluid.

As described in Materials and Methods, diaphragms from uninjected mice or after PBS injection showed no staining with trypan blue (Figure 10). In contrast, 3 days after injection of 200 μg of long or mixed asbestos fibers, large areas of trypan blue staining were seen (Figure 11). The distribution of trypan blue staining of the diaphragm was mapped by stereomicroscopy between 3 hours and 14 days. After 3 hours, areas of blue staining measuring $1.5 \times 10\ \mu$ to $2 \times 20\ \mu$ were seen in the lacunar regions. As more

fibers accumulated on the surface of the diaphragm, the areas of stained cells increased in size and in number. After 6 hours, 29 blue areas up to 3.5 × 35 μ in size were found in the muscular region of the diaphragm and along the musculotendinous junction. At this time, some staining was also evident in the submesothelial layer in the lacunar regions. This most likely represents penetration of trypan blue into lymphatics. After 24 hours, the stained areas were even larger (19 × 41 μ). Multiple layers of blue cells were seen at this time. Maximal staining with trypan blue occurred 3 days after injection: at 3.7-fold magnification, 83% of the surface area of the diaphragm was stained. By 7 days, the extent of trypan blue staining was reduced. Blue patches, 0.3 × 20 μ to 12 × 74 μ in area, surrounded some of the fiber clusters. After 14 days, very little trypan blue staining was seen; the diaphragm was similar to the one shown in Figure 10.

Staining of mesothelial cells in this viability assay was documented by surface imprints of the diaphragm prepared 3 days after injection of long asbestos fibers. The mosaic arrangement of the surface mesothelium with blue staining is shown in Figure 12. This staining pattern is not due to endocytosis of trypan blue by the numerous macrophages in these lesions because only 2.4% of the free peritoneal macrophage population collected 3 days after injection of asbestos took up trypan blue under these assay conditions.

The intensity and distribution of trypan blue uptake was very different after injection of 200 μg of short asbestos fibers. After 3 hours only 3 cell clusters were stained in the lacunar regions. After 3 days, 3 areas in the muscular region and 2 in the musculotendinous junction were stained. These areas were only 0.1 × 0.2 μ in size. Similarly, 3 days after injection of silica particles, only 3 small areas were stained with trypan blue. By 7 days after injection of short asbestos fibers or silica particles, no trypan blue staining was seen. During the same time period, no trypan blue staining was seen after injection of PBS, titanium dioxide, or the soluble irritant, thioglycollate broth.

The extent of trypan blue staining of the mesothelium was paralleled by recovery of lactate dehydrogenase (LDH) activity in the peritoneal lavage fluid measured as described in Materials and Methods. The time course of this release is shown in Figure 13. After injection of 200 μg of long asbestos fibers (open cir-

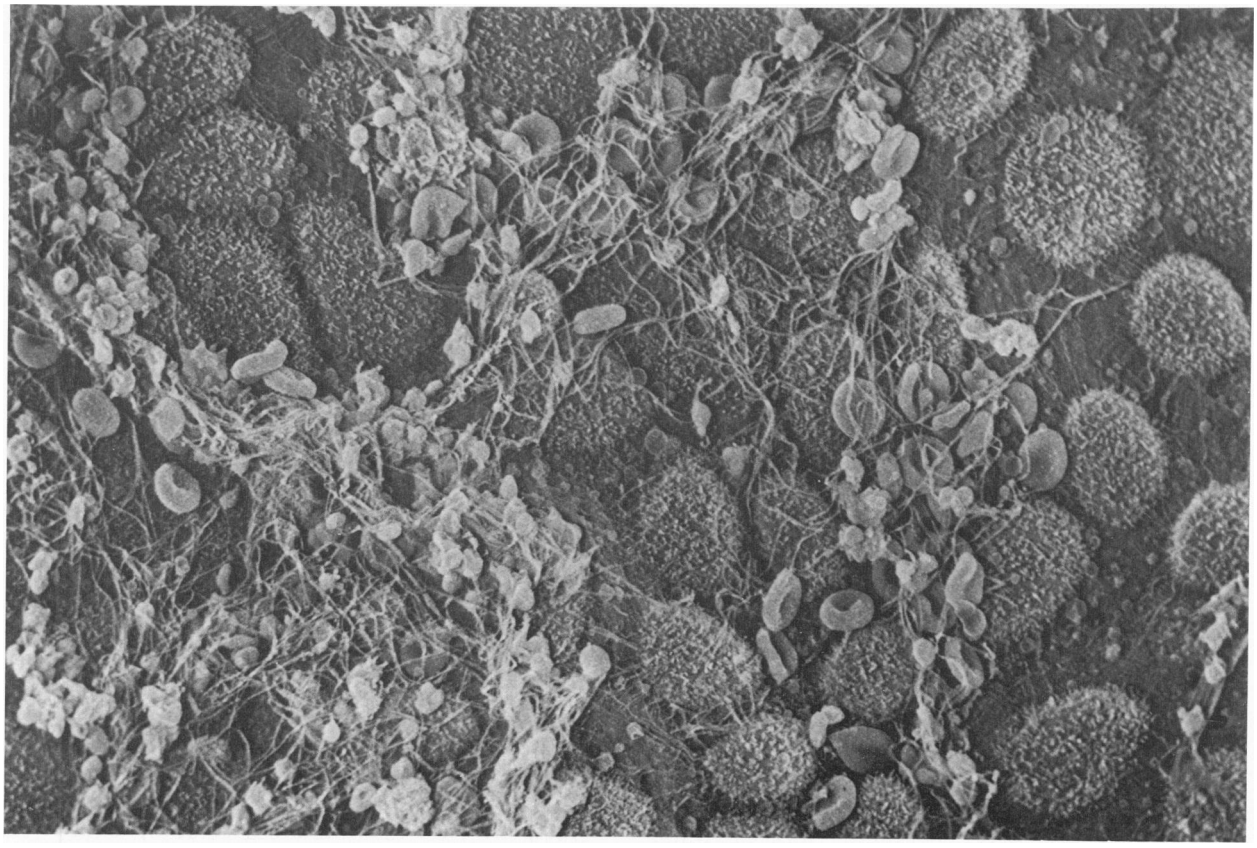

Figure 6—Scanning electron micrograph of the surface of the lacunar region of a diaphragm removed 3 hours after injection of 200 μg of native (mixed lengths) crocidolite asbestos fibers. The cuboidal mesothelial cells are covered by a meshwork of fibrin, red blood cells, and platelets. (×1660)

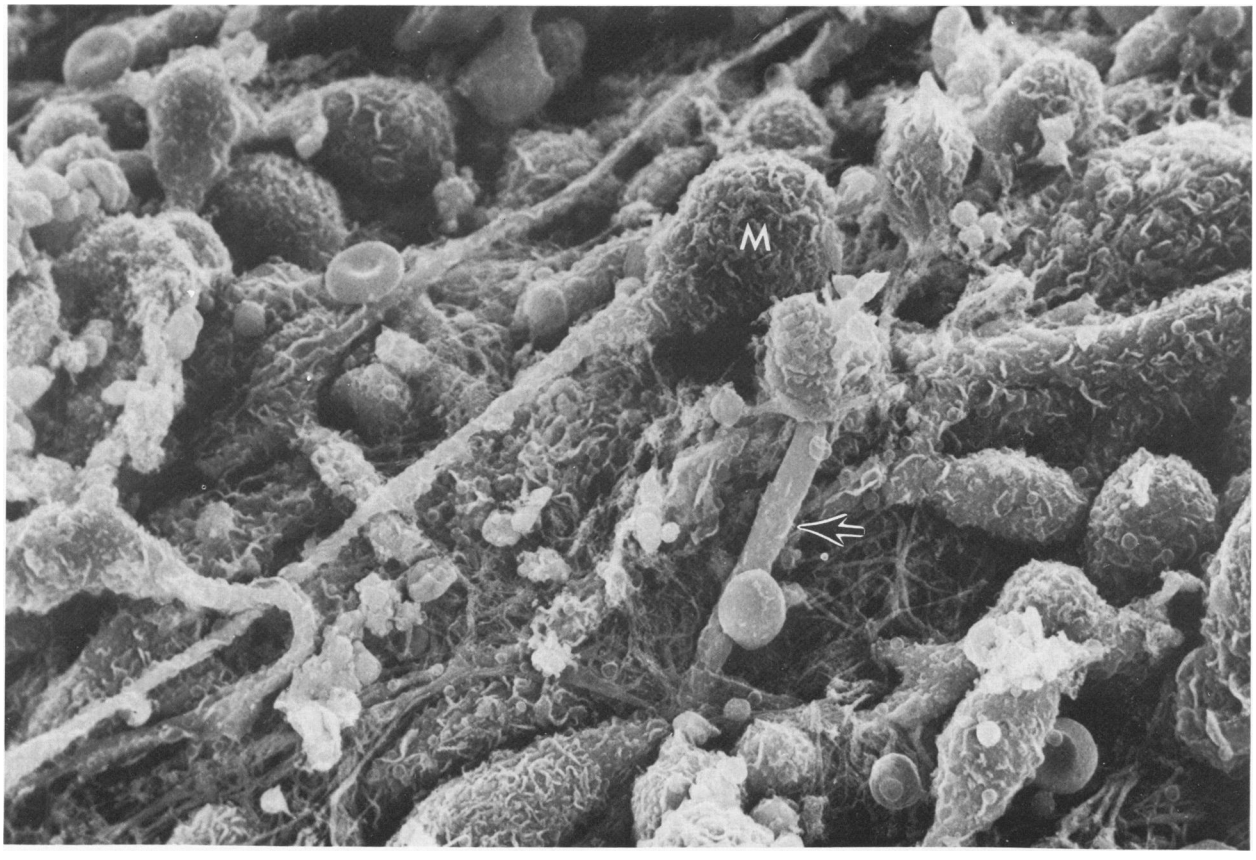

Figure 7—Scanning electron micrograph of the surface of a fiber cluster on a diaphragm removed 3 days after injection of 200 μg of long asbestos fibers. The mesothelial cells are almost completely covered by macrophages (*M*) with ruffled surfaces containing long, straight asbestos fibers (*arrows*). Cell debris and occasional red blood cells are also present. (×2080)

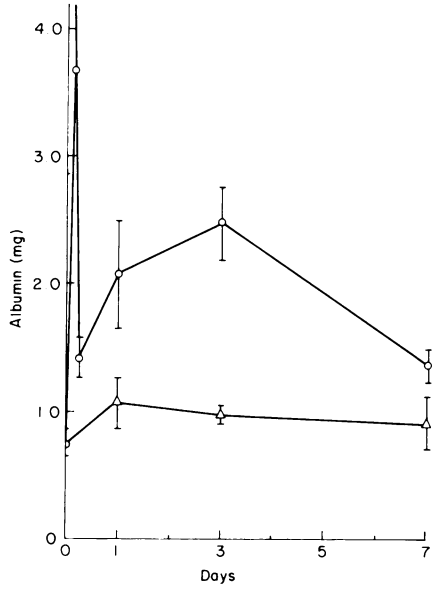

Figure 8—Recovery of albumin in peritoneal lavage fluid after injection of asbestos fibers. At intervals between 3 hours and 7 days after injection of 200 μg of long (○) or short (△) crocidolite asbestos fibers, the albumin content of peritoneal lavage fluid was determined as described in Materials and Methods. The *points* are the means obtained from 3 animals; the *bars* indicate the standard deviations.

cles), there is a small peak of LDH activity at 3 hours, with a larger peak after 3 days. After 21 days, the levels had returned to control values. In contrast, a slight elevation of LDH activity was found between 3 and 7 days after injection of 200 μg of short asbestos fibers (open triangles). No increased LDH activity was

Table 3—Albumin Recovery in Peritoneal Lavage Fluid

Injection	Total μg recovered ± SEM
None	729 ± 108
PBS	454 ± 34
Thioglycollate	993 ± 107
TiO_2	670 ± 40
SiO_2	478 ± 66
Short fibers	977 ± 69*
Long fibers	2486 ± 292†

*$P < 0.05$ for short fibers versus long fibers.

†$P < 0.01$ for long fibers versus PBS injection.

Peritoneal lavage fluid was obtained after injection of 8 ml of PBS intraperitoneally. Three mice in each group were sacrificed 3 days following injection as indicated. Albumin content was measured as described in Materials and Methods. Statistical significance was determined with the Student *t* test.

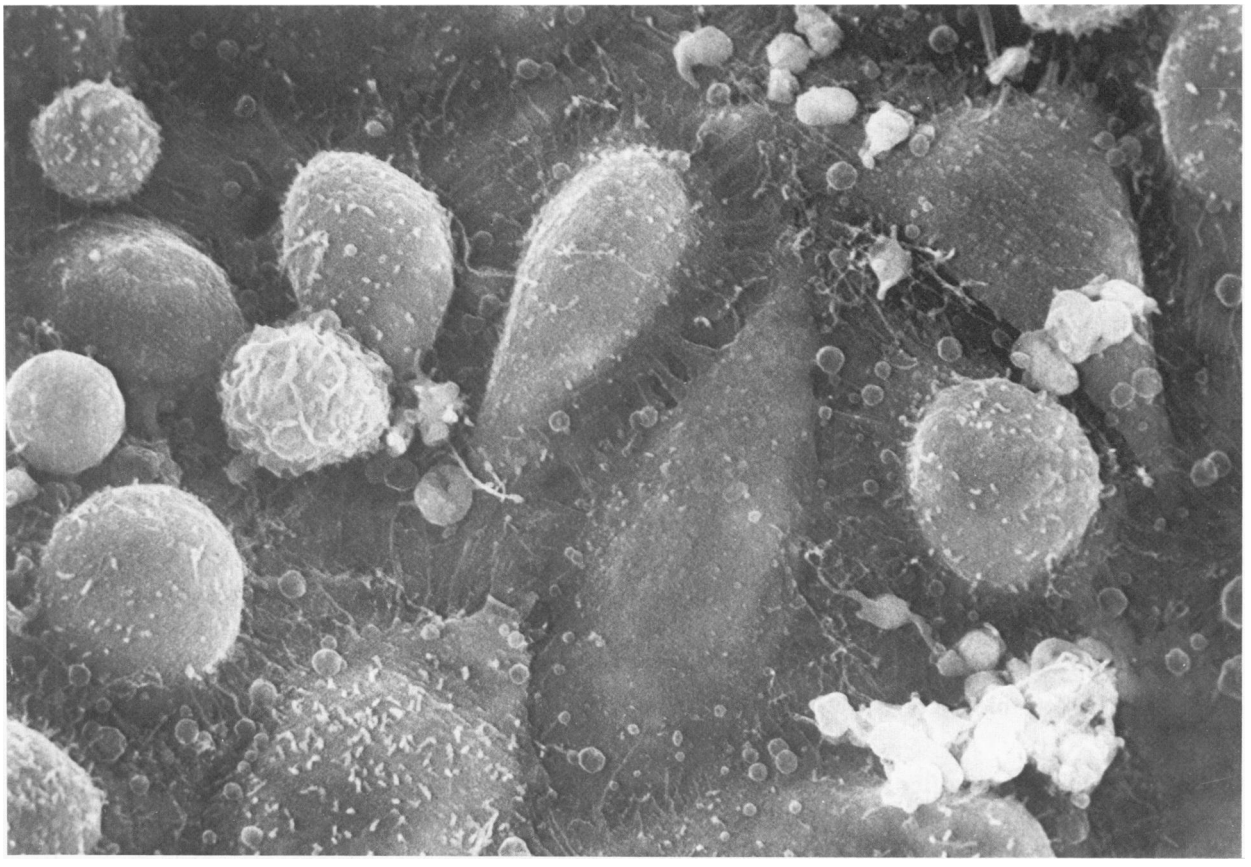

Figure 9—Scanning electron micrograph of the mesothelial surface of a diaphragm removed 12 hours after injection of 200 μg of long crocidolite asbestos fibers. The mesothelial cells are round and swollen with loss of their surface microvilli and numerous surface blebs. The tight intercellular junctions have partially separated. (×2080)

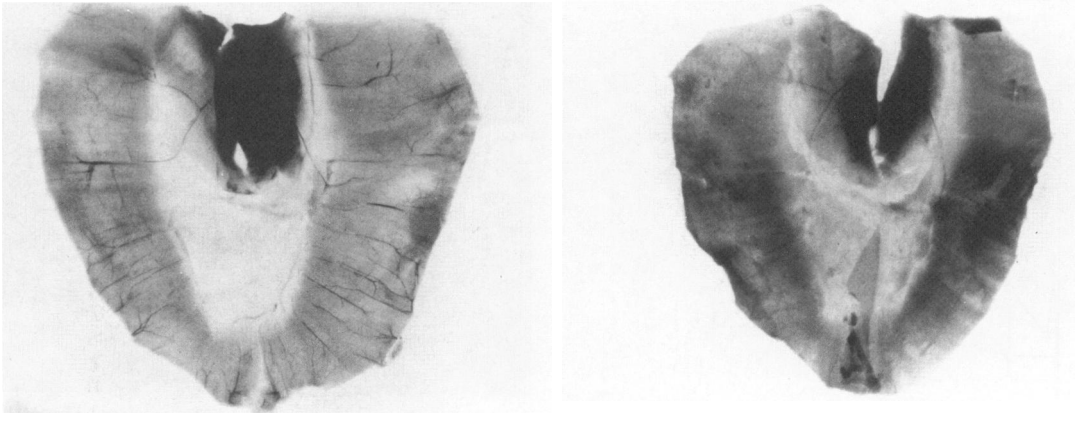

Figure 10—Light micrograph of a diaphragm removed from an uninjected mouse and stained with trypan blue as described in Materials and Methods. As visualized with a dissecting stereomicroscope, the original specimen was not stained blue. In this black-and-white photograph, the central tendinous region is almost white and the surrounding muscular region is gray. The black area at the top of the photograph is the transected psoas muscles, which are stained during this procedure. (×8.3) **Figure 11**—Light micrograph of a diaphragm removed 3 days after injection of 200 μg of long crocidolite asbestos fibers and stained with trypan blue as described in Materials and Methods. As visualized with a dissecting stereomicroscope, the central tendinous region, areas of the muscular region, and the falciform ligament stained blue. These areas are dark gray or black in this photograph. As seen under a dissecting stereomicroscope, only the surface cells or occasionally the submesothelial lymphatics took up trypan blue dye. The underlying skeletal muscle fibers of the diaphragm were not stained. (×8.3)

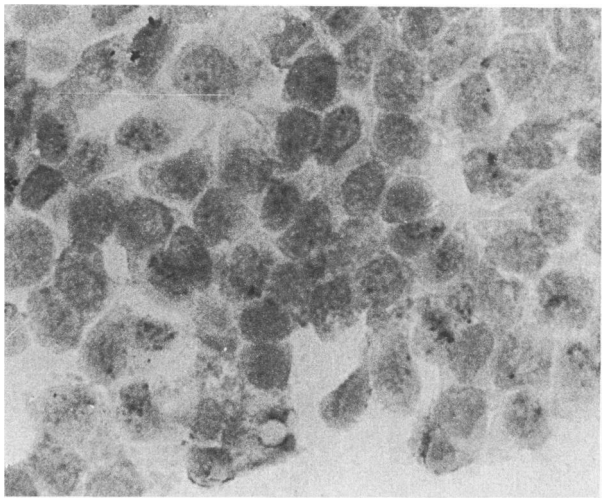

Figure 12—Surface imprint of an area of mesothelial cells stained with trypan blue. This preparation was obtained 3 days after injection of 200 μg of long asbestos fibers as described in Materials and Methods. This monolayer of cells shows diffuse blue staining of the cytoplasm and nucleus, which appear gray in this photograph. Unstained cells appear white under these conditions. (×938)

found 3 days after injection of PBS, titanium dioxide or silica particles, or thioglycollate broth (Table 4).

Mesothelial Regeneration after Injection of Asbestos Fibers

The restoration of the mesothelium was studied by scanning electron microscopy and by autoradiography after pulse-labeling with ^{3}H-thymidine. Immature mesothelial cells were identified morphologically at the periphery of fiber clusters beginning 3 days after injection of 200 μg of mixed or long asbestos fibers. The surface morphology of regenerating mesothelial cells has been described in detail by Whitaker and

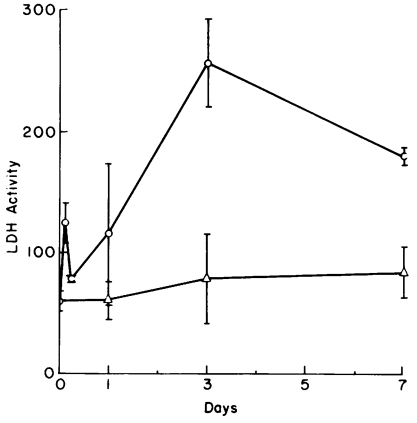

Figure 13—Recovery of LDH activity in peritoneal lavage fluid after injection of asbestos fibers. At intervals between 3 hours and 7 days after injection of 200 μg of long (○) or short (△) crocidolite asbestos fibers, the peritoneal lavage fluid was collected and assayed for lactate dehydrogenase activity as described in Materials and Methods. The *points* are the means obtained from 3 animals; the *bars* indicate the standard deviations.

Table 4—LDH Activity Recovered in Peritoneal Lavage Fluid

Injection	Total units ± SEM
None	59 ± 8
PBS	44 ± 13
Thioglycollate	48 ± 6
TiO_2	55 ± 5
SiO_2	48 ± 3
Short fibers	79 ± 37*
Long fibers	257 ± 37†

*$P < 0.05$ for short fibers versus long fibers.
†$P < 0.05$ for long fibers versus PBS injection.
Peritoneal lavage fluid was collected from 3 mice in each group 3 days after injection as described in Table 3. LDH activity was measured as described in Materials and Methods. Statistical significance was determined with the Student *t* test.

Papadimitriou (1985)[58] after wounding of the parietal peritoneum of the rat scrotal sac. These immature mesothelial cells are shown in Figure 14. Round cells with short microvilli and several filopodia migrate from the periphery of the fiber cluster inward. As these cells flatten out to restore the mesothelial surface over the fiber clusters, the surface microvilli be-

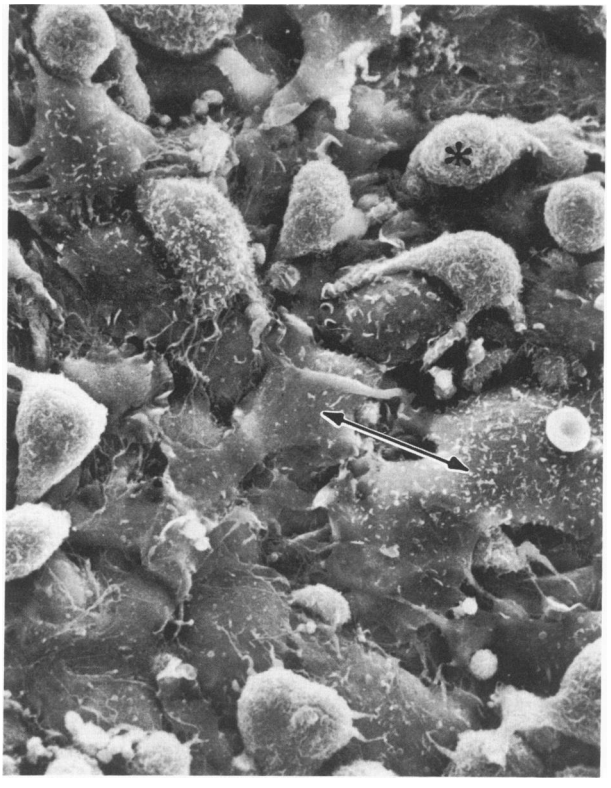

Figure 14—Scanning electron micrograph of a fiber cluster on the diaphragm removed 7 days after injection of 200 μg of long asbestos fibers. The cells covering the fiber cluster are mesothelial cells at various stages of regeneration. At the periphery of the photograph are round cells covered with numerous short microvilli (*). Some of these less mature cells have slender filopodia. In the center of the photograph, the cells are flattened with sparse microvilli (as indicated by the *arrows*). A variety of junctional contacts is seen ranging from thin intercellular bridges to tight junctions characteristic of mature, flat mesothelial cells. (×880)

come sparse. By comparison, injured mesothelial cells shown in Figure 9 with loss of microvilli are rounded and swollen, with surface blebs. The flattened, regenerating cells form thin filamentous extensions, which eventually interdigitate until tight intercellular junctions are reestablished after 14 days (Figure 15). At this time, the regenerated cells again have numerous thin microvilli, but they are more cuboidal than mature, flat mesothelium. After 21 days, most of the mesothelium was restored especially in the lacunar regions. Clusters of fibers were still visible at the musculotendinous junction under the dissecting stereomicroscope. When examined by scanning electron microscopy (Figure 16), the center of the fiber cluster was almost completely covered by flattened mesothelial cells. A single protruding fiber is seen in the lower half of this lesion. Restoration of the mesothelium is not yet complete. This lesion is still surrounded by macrophages and round mesothelial cells. Even 6 months after a single injection of mixed asbestos fibers, macrophages and immature mesothelial cells are scattered on the surface, covering several layers of fibroblasts and macrophages, as shown in Figure 17.

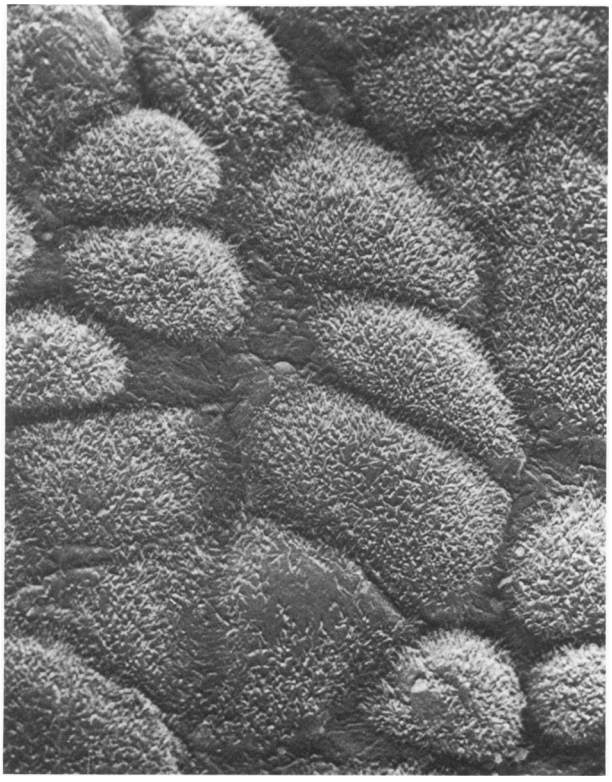

Figure 15—Scanning electron micrograph of a fiber cluster on a diaphragm removed 14 days after injection of 200 μg of long asbestos fibers. The mesothelium has been restored by cuboidal and partially flattened cells with numerous, thin microvilli. The tight intercellular junctions are almost completely reestablished. (×1120)

The proliferative response of the mesothelium after injection of asbestos fibers was also studied by means of autoradiography. At various times after injection, mice were injected intraperitoneally with ^{3}H-thymidine 1 hour before sacrifice. The diaphragms were dissected, coated with photographic emulsion, and developed after a 1-week exposure as described in Materials and Methods. The number of labeled nuclei per square centimeter was determined by means of a dissecting stereomicroscope at 70× magnification. As shown in Figure 18, numerous labeled nuclei were seen on the muscular region of the diaphragm 3 days after injection of long asbestos fibers. In contrast, very few labeled nuclei were seen after injection of silica particles (Figure 19). The incorporation of the isotope by surface mesothelial cells was confirmed by a cross-section of the diaphragm photographed under the light microscope as shown in Figure 20. The areas of ^{3}H-thymidine incorporation corresponded to regions of trypan blue staining seen after 3 days (Figure 11): the lacunar regions were labeled most densely with little ^{3}H-thymidine incorporation in the central tendinous region. The distribution of ^{3}H-thymidine labeling around fiber clusters after 3 days was similar to the location of immature mesothelial cells as visualized by scanning electron microscopy: labeled cells first appeared at the periphery of fiber clusters, then moved in toward the center of these lesions. After 7 days, there was heavy labeling over most of the muscular region of the diaphragm. Focal areas of ^{3}H-thymidine incorporation persisted even after 14 days. This was observed over aggregates of fibers along the musculotendinous junction corresponding to the lesions studied by scanning electron microscopy as shown in Figure 16.

Some ^{3}H-thymidine incorporation was seen 3 days after injection of short asbestos fibers (open triangles in Figure 21); however, this was almost two orders of magnitude less than the labeling seen 7 days after injection of long asbestos fibers (open circles). Similarly, a low level of ^{3}H-thymidine incorporation was found 3 days after injection of thioglycollate broth or silica, compared with almost no labeling in response to injection of PBS or titanium dioxide particles (Table 5).

Discussion

These experiments compared the acute morphologic reactions of the mesothelium to mineral particles of different sizes and composition. Long asbestos fibers were not cleared efficiently through lymphatic stomata and were trapped at the mesothelial surface. Short asbestos fibers or spherical mineral particles

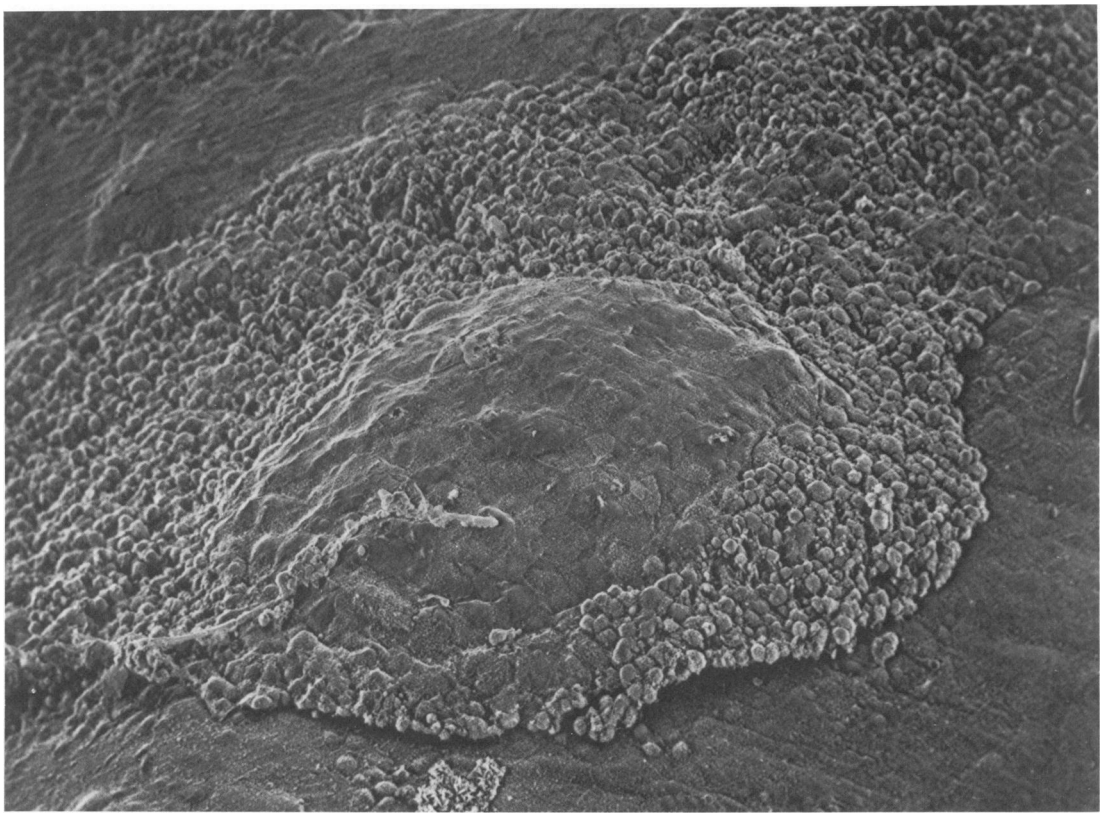

Figure 16—Scanning electron micrograph of a cluster of asbestos fibers at the musculotendinous junction of a diaphragm removed 5 weeks after a single injection of 200 μg of native (mixed lengths) crocidolite asbestos fibers. The central area of the fiber cluster is covered by mature, flat mesothelial cells. These are surrounded by round, regenerating mesothelial cells and macrophages. (×255)

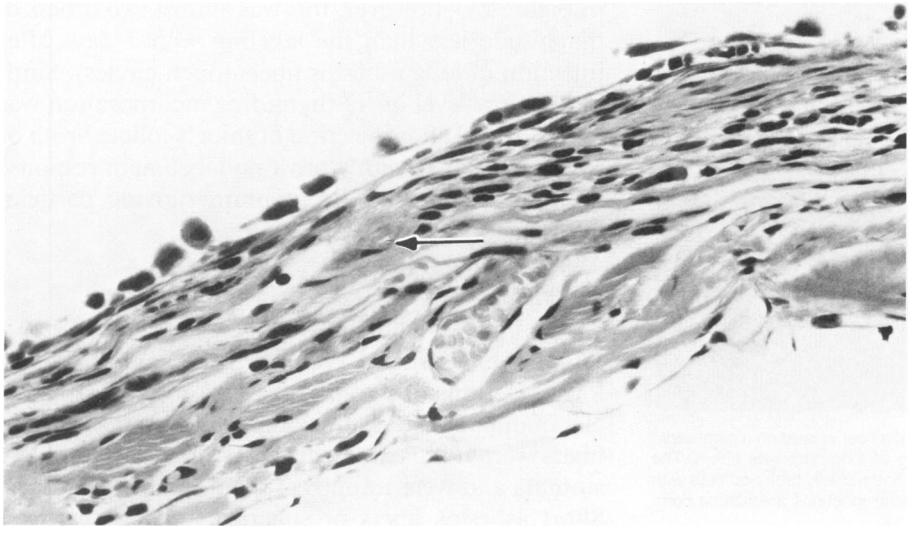

Figure 17—Light micrograph of a fiber cluster seen in cross-section on the muscular region of a diaphragm removed 6 months after a single injection of 200 μg of native (mixed lengths) crocidolite asbestos fibers. A single asbestos fiber as indicated by the *arrow* is present in the thickened submesothelial cell layer. This lesion is covered by round and partially flattened mesothelial cells. (×938)

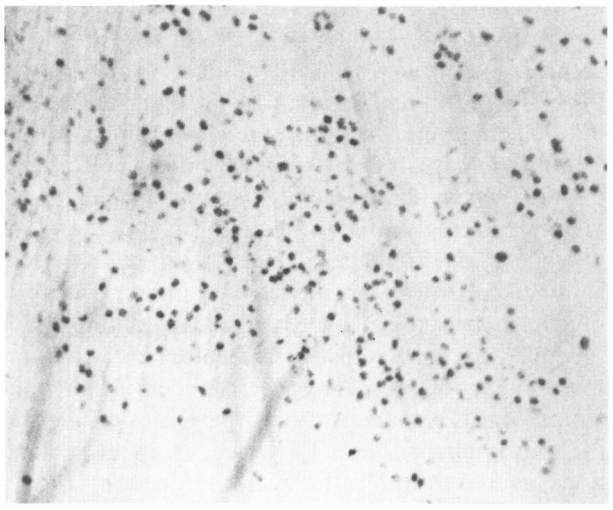

Figure 18—Autoradiograph of the surface of the muscular region of a diaphragm removed 3 days after injection of 200 μg of long asbestos fibers. As seen under a dissecting stereomicroscope, the nuclei which have incorporated ^{3}H-thymidine appear as black dots. (×700)

were easily cleared through lymphatic stomata. At the sites of trapped asbestos fibers, an intense inflammatory reaction developed, characterized by accumulation of activated macrophages after 3 days. Localized injury of the mesothelium was found in response to long or mixed lengths of crocidolite asbestos fibers. The mesothelial lining was partially restored by regeneration after 14–21 days. The localized nature of these reactions produced only by long or mixed lengths of asbestos fibers may be a critical factor that contributes to the subsequent emergence of mesotheliomas. The mechanisms responsible for the localization of asbestos fibers, the inflammatory reaction, and mesothelial injury and repair and the relationship between these events and the development of mesotheliomas will be discussed next.

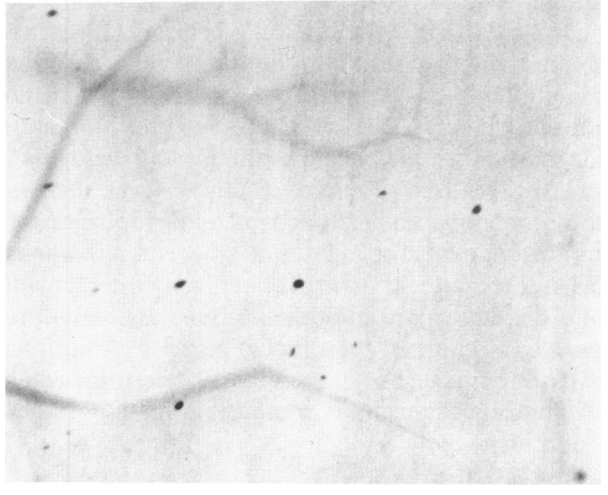

Figure 19—Autoradiograph of the surface of the muscular region of a diaphragm removed 3 days after injection of 200 μg of silica particles. In this photograph taken under a dissecting stereomicroscope, only a few labeled nuclei are seen. (×700)

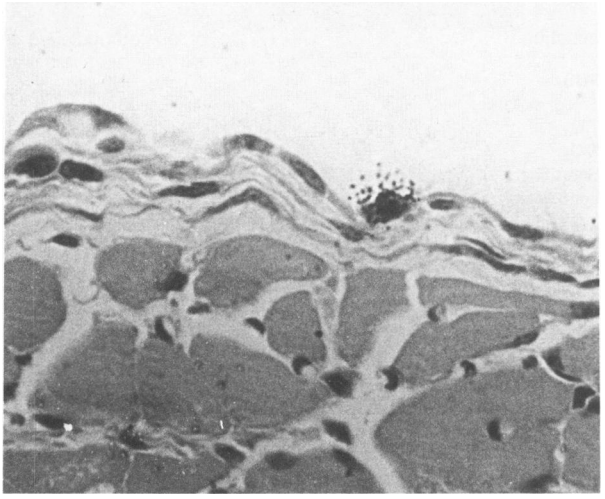

Figure 20—Light micrograph of a cross-section through the muscular region of a diaphragm removed 3 days after injection of 200 μg of long asbestos fibers. This diaphragm was processed for autoradiography as described in Materials and Methods, then sectioned for routine histology. The labeled nucleus of a surface mesothelial cell is seen above the cross-sectioned skeletal muscle fibers. Only flattened cells at the surface of the diaphragm were labeled under these conditions; no ^{3}H-thymidine incorporation was found over macrophages. (×1100)

Localization of Asbestos Fibers

The clearance of long asbestos fibers from the peritoneum appears to be limited by the diameter of lymphatic stomata in the lacunar regions of the dia-

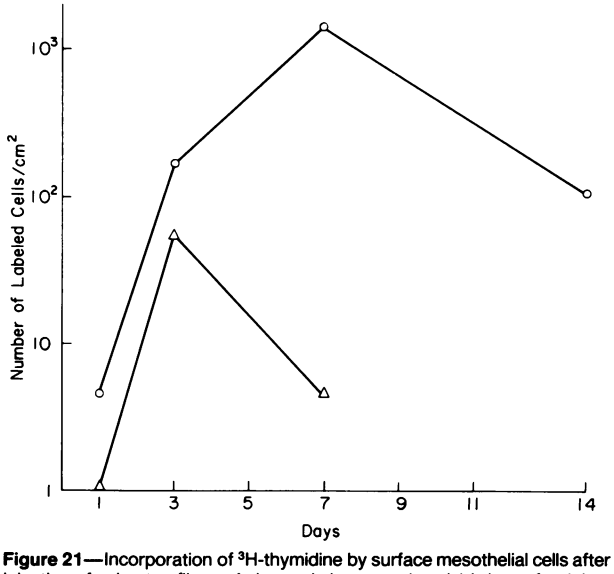

Figure 21—Incorporation of ^{3}H-thymidine by surface mesothelial cells after injection of asbestos fibers. At intervals between 1 and 14 days after injection of long (○) or short (△) asbestos fibers, the diaphragms were removed and processed for autoradiography as described in Materials and Methods. Each point is the average of the number of labeled cells per square centimeter on the surface of the diaphragms removed from 2 animals at each time point.

Table 5—^{3}H-Thymidine Incorporation by Mesothelial Cells

Injection	No. of labeled nuclei/sq cm
PBS	1.0
Thioglycollate	38.2
TiO_2	1.5
SiO_2	41.9
Short fibers	55.6
Long fibers	168.4

Three days after injection as indicated, mice were injected intraperitoneally with ^{3}H-thymidine for 1 hour before sacrifice. The diaphragms were dissected and prepared for autoradiography as described in Materials and Methods. The number of labeled nuclei per square centimeter on the peritoneal surface was counted with a dissecting stereomicroscope at 70× magnification calibrated with a 1-sq mm eyepiece grid. The numbers are the average of the labeling indices counted from at least 2 animals per experimental group in separate experiments.

phragm. Several questions regarding the clearance of fibers from the peritoneum were not resolved by these experiments. First, how do particulates reach the lymphatic stomata? Are they cleared individually or transported by peritoneal macrophages? A similar consideration applies to translocation of inhaled particulates to thoracic lymph nodes. Recent experiments suggest that alveolar macrophages transport particulates to hilar and tracheobronchial lymph nodes.[59,60] Second, regardless of the mode of transport, what signals guide the migration of particulates from the peritoneum? Is this movement caused by negative pressure in the lymphatic network, or are specific chemotactic fibers generated by the interaction between mineral particles and the peritoneal lining fluid or resident macrophages? Again, a similar question can be asked about removal of particulates from the lung. There is evidence that asbestos fibers generate chemotactic peptides from alveolar lining fluid.[61,62] Following inhalation, asbestos fibers and alveolar macrophages have been shown to accumulate selectively at bifurcations of alveolar ducts[63] and around bronchioles,[64] presumably in response to chemotactic factors. An analogous mechanism may operate at the mesothelial surface following intraperitoneal injection of asbestos fibers: long fibers are trapped at the stomata of lymphatics and stimulate release of chemotactic factors, leading to accumulation of macrophages at these sites.

The Inflammatory Response and Mesothelial Injury

The inflammatory reaction to asbestos fibers is dominated by the presence of nonspecifically activated macrophages which can be identified histologically and by histochemical assays for acid phosphatase activity and binding of *Griffonia* lectin as early as 12–24 hours after injection (Branchaud et al, manuscript in preparation). Accumulation of nonspecifically activated macrophages in the peritoneal cavity is not in itself sufficient to produce the extent of mesothelial cell injury seen after injection of asbestos fibers. Injection of thioglycollate broth, a soluble irritant, elicits monocytes from the blood and leads to a 10-fold increase in the number of nonspecifically activated macrophages recovered by peritoneal lavage. However, thioglycollate injection did not cause adherence of macrophages to the mesothelium or mesothelial cell injury, as indicated by uptake of trypan blue or increased LDH activity recovered in the peritoneal lavage fluid. A distinctive feature of the inflammatory reaction evoked by asbestos fibers is the localization of this response around aggregates of fibers at the mesothelial surface. Fibers persist at these locations, even 6 months after a single injection. The retention of asbestos fibers at these sites appears to be the stimulus for the maintenance of the inflammatory reaction characterized by nonspecifically activated macrophages. This inflammatory reaction is accompanied by mesothelial cell injury and regeneration. In contrast, thioglycollate broth is a soluble, digestible irritant; and the inflammatory response subsides after 7 days, without causing injury.

The persistence of this inflammatory reaction at the sites of fiber clusters suggests that mediators released from nonspecifically activated macrophages may be responsible for perpetuating both the inflammatory reaction[65] and tissue injury. Activated macrophages release a wide variety of chemical mediators, some of which are responsible for initiating inflammation[66] and tissue injury at other sites. The local persistence of asbestos fibers probably serves as a continual stimulus for release of these mediators from activated macrophages. The most likely mediators responsible for tissue damage are reactive oxygen metabolites, especially the hydroxyl radical.[29] Release of reactive oxygen metabolites from nonspecifically activated macrophages has been detected[28,29] and implicated in the cytotoxicity of asbestos fibers *in vitro*.[29,30] A similar mechanism may occur at the mesothelial surface *in vivo*: localized release of reactive oxygen metabolites from nonspecifically activated macrophages may injure both macrophages and adjacent mesothelial cells. Alternatively, asbestos fibers may interact with and directly injure mesothelial cells, as shown previously in cultured mesothelial cells.[21,22] Additional experiments must be carried out to determine which of these mechanisms is responsible for mesothelial cell injury *in vivo*.

Mesothelial Regeneration

After the mesothelium is injured, regardless of the nature of the initial insult, regeneration can occur.[67]

The pathway leading to restoration of the mesothelial lining is controversial. Regeneration may be accomplished by proliferation of uninjured cells at the periphery of the wound, attachment and proliferation of freely floating mesothelial cells,[58] or differentiation of submesothelial cells.[68,69] One or more of these pathways may lead to mesothelial regeneration following injury produced by asbestos fibers. With this irritant, an additional mechanism may also contribute to stimulation of growth. Unlike direct thermal injury of the mesothelium studied by Whitaker and Papadimitriou (1985),[58] asbestos fibers are surrounded by activated macrophages. These cells release a variety of growth factors for mesenchymal cells[66]; one or more of these factors may also stimulate mesothelial cell proliferation. Persistent release of these growth factors may be responsible for the continuing proliferation of mesothelial cells around aggregates of asbestos fibers.

Injury to the mesothelium appears to be a prerequisite for stimulation of mesothelial cell proliferation. In the absence of disruption of the mesothelial monolayer, there is very little mesothelial cell proliferation.[67] The mesothelial lining is exposed to macrophages activated by injection of thioglycollate broth; however, as shown in this paper, the mesothelium remained intact and was not stimulated to proliferate. In contrast with the other mineral dusts studied in this experimental model, asbestos fibers have the unique property of causing injury followed by regeneration of the mesothelial lining. In contrast to direct physical injury to the mesothelium,[58] asbestos fibers also provoke a persistent inflammatory reaction. This unique combination of proliferative and inflammatory reactions to asbestos fibers may contribute to their carcinogenicity.

In this experimental model using a single injection of asbestos fibers, mesothelial regeneration, although incomplete after 6 months, was the predominant response of the peritoneal lining. No fibrotic[70] or calcified plaques were produced after a single injection of 200 μg of fibers, although it is well known that human exposure to asbestos produces these lesions in the pleural lining.[71] The earliest response to injection of asbestos fibers was focal hemorrhage and fibrin deposition. Organization of fibrin is hypothesized to be the initial stimulus leading to pleural adhesions and fibrosis.[72] In this experimental model, dissolution, rather than organization, of fibrin was observed. Two different mechanisms may lead to fibrinolysis in this system. Peritoneal macrophages elicited by injection of asbestos have been shown to produce plasminogen activator,[73] which can lead to clot lysis. In addition, regenerating mesothelial cells also have fibrinolytic activity.[74] Therefore, after acute mesothelial injury produced by this dose of asbestos fibers, fibrinolysis predominates. Additional experiments must be conducted to determine whether fibrin organization, rather than dissolution, characterizes chronic or repeated exposure to asbestos fibers.

Proposed Mechanism Leading to Mesotheliomas

The potential roles of fiber localization, accumulation of macrophages, and mesothelial injury and regeneration in the development of mesotheliomas are summarized in Figure 22. Long asbestos fibers are trapped at lymphatic stomata and stimulate accumulation of nonspecifically activated macrophages at the mesothelial surface. This observation does not completely eliminate a role for short asbestos fibers in the induction of mesotheliomas. After injection of native crocidolite asbestos containing mixed fiber lengths, short fibers were also found within the aggregates of long fibers. Alternatively, if the lymphatics were occluded by large numbers of short fibers or after a prolonged period, short fibers may also accumulate at the mesothelial surface and produce mesotheliomas. Asbestos fibers, either directly or indirectly via reactive oxygen metabolites released from activated macrophages, injure adjacent mesothelial cells. Mesothelial cell injury may include oxidative damage to DNA, leading to mutations,[34] or chromosomal damage secondary to cytoskeletal disruption.[18] Injury to the mesothelium can be partially repaired after a single exposure to asbestos fibers. However, repeated episodes of mesothelial injury and regeneration, possibly stimulated by growth factors released from macrophages, may lead to the emergence of populations of cells with altered growth properties. One or more of these populations may give rise to a mesothelioma.

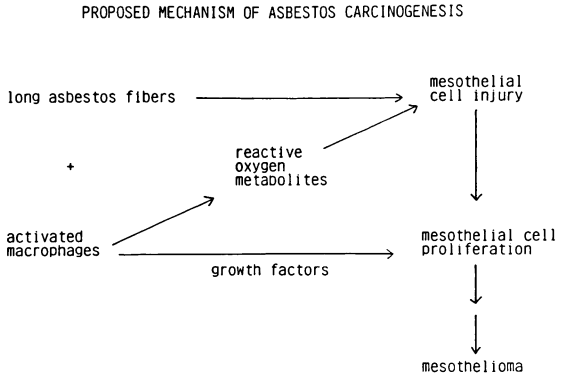

Figure 22—Reactive oxygen metabolites released from activated macrophages are hypothesized to injure mesothelial cells. Macrophage-derived growth factors may stimulate mesothelial cell proliferation and promote the development of mesotheliomas.

References

1. Craighead JE, Mossman BT: The pathogenesis of asbestos-associated diseases. N Engl J Med 1982, 306:1446–1455
2. Davis JMG: The pathology of asbestos related disease. Thorax 1984, 39:801–808
3. Stanton MF, Layard M, Tegeris A, Miller E, May M, Kent E: Carcinogenicity of fibrous glass: Pleural response in the rat in relation to fiber dimension. J Natl Cancer Inst 1977, 58:587–603
4. Lee KP, Trochimowica HJ, Reinhardt CF: Pulmonary response of rats exposed to titanium dioxide (TiO_2) by inhalation for two years. Toxicol Appl Pharmacol 1985, 79:179–192
5. Adamson IYR, Bowden DH: Crocidolite-induced pulmonary fibrosis in mice: cytokinetic and biochemical studies. Am J Pathol 1986, 122:261–267
6. Bowden DH, Adamson IYR: The role of cell injury and the continuing inflammatory response in the generation of silicotic pulmonary fibrosis. J Pathol 1984, 144:149–161
7. Wagner JC, Berry G, Skidmore JW, Timbrell V: The effects of the inhalation of asbestos in rats. Br J Cancer 1974, 29:252–269
8. Wagner JC, Berry G: Mesotheliomas in rats following innoculation with asbestos. Br J Cancer 1969, 23:567–581
9. Wagner JC, Berry G, Timbrell V: Mesotheliomata in rats after inoculation with asbestos and other materials. Br J Cancer 1973, 28:173–185
10. Stanton MF, Layard M, Tegeris A, Miller E, May M, Morgan E, Smith A: Relation of particle dimension to carcinogenicity in amphibole asbestoses and other fibrous minerals. J Natl Cancer Inst 1981, 67:965–975
11. Monchaux G, Bignon J, Jaurand MC, Lafuma J, Sebastien P, Masse R, Hirsch A, Goni J: Mesotheliomas in rats following inoculation with acid-leached chrysotile asbestos and other mineral fibers. Carcinogenesis 1981, 2:229–236
12. Chamberlain M, Tarmy EM: Asbestos and glass fibres in bacterial mutation tests. Mutat Res 1977, 43:159–164
13. Huang SL, Saggioro D, Michelman H, Malling HV: Genetic effects of crocidolite asbestos in Chinese hamster lung cells. Mutat Res 1978, 57:225–232
14. Reiss B, Solomon S, Tong C, Levenstein M, Rosenberg SH, Williams M: Absence of mutagenic activity of three forms of asbestos in liver epithelial cells. Environ Res 1982, 27:389–397
15. Fornace AJ, Jr.: Detection of DNA single-strand breaks produced during the repair of damage by DNA-protein cross-linking agents. Cancer Res 1982, 42:145–149
16. Denizeau F, Marion M, Chevalier G, Cote MG: Inability of chrysotile asbestos fibers to modulate the 2-acetylaminofluorene-induced UDS in primary cultures of rat hepatocytes. Mutat Res 1985, 155:83–90
17. Sincock A, Seabright M: Induction of chromosome changes in Chinese hamster cells by exposure to asbestos fibres. Nature 1975, 257:56–57
18. Barrett JC, Hesterberg TW, Oshimura M, Tsutsui T: Role of chemically induced mutagenic events in neoplastic transformation of Syrian hamster embryo cells, Carcinogenesis. Vol 9. Edited by JC Barrett, RW Tennant. New York, Raven Press, 1985, pp 123–137
19. Jaurand M-C, Kaplan H, Thiollet J, Pinchon M-C, Bernaudin J-F, Bignon J: Phagocytosis of chrysotile fibers by pleural mesothelial cells in culture. Am J Pathol 1979, 94:529–538
20. Rajan KT, Wagner JC, Evans PH: The response of human pleura in organ culture to asbestos. Nature 1972, 238:346–347
21. Lechner JF, Tokiwa T, LaVeck M, Benedict WF, Banks-Schlegel S, Yeager H, Jr, Banerjee A, Harris CC: Asbestos-associated chromosomal changes in human mesothelial cells. Proc Natl Acad Sci USA 1985, 82:3884–3888
22. Jaurand MC, Kheuang L, Magne L, Bignon J: Chromosomal changes induced by chrysotile fibres or benzo-3,4-pyrene in rat pleural mesothelial cells. Mutat Res 1986, 169:141–148
23. Mossman BT, Ley B, Kessler JB, Craighead JE: Interaction of crocidolite asbestos with hamster respiratory mucosa in organ culture. Lab Invest 1977, 36:131–139
24. Landesman JM, Mossman BT: Induction of ornithine decarboxylase in hamster tracheal epithelial cells exposed to asbestos and 12-0-tetradecanoyl phorbol-13-acetate. Cancer Res 1982, 42:3669–3675
25. Woodworth CD, Mossman BT, Craighead JE: Induction of squamous metaplasia in organ cultures of hamster trachea by naturally occurring and synthetic fibers. Cancer Res 1983, 43:4906–4912
26. Paterour MJ, Bignon J, Jaurand MC: In vitro transformation of rat pleural mesothelial cells by chrysotile fibres and/or benzo(a)pyrene. Carcinogenesis 1985, 6:523–529
27. Chamberlain M: The influence of mineral dusts on metabolic co-operation between mammalian cells in tissue culture. Carcinogenesis 1982, 3:337–339
28. Donaldson K, Cullen RT: Chemiluminescence of asbestos-activated macrophages. Br J Exp Pathol 1984, 65:81–90
29. Goodglick LA, Kane AB: Role of reactive oxygen metabolites in crocidolite asbestos toxicity to mouse macrophages. Cancer Res 1986, 46:5558–5566
30. Mossman BT, Marsh JP, Shatos MA: Alteration of superoxide dismutase activity in tracheal epithelial cells by asbestos and inhibition of cytotoxicity by antioxidants. Lab Invest 1986, 54:204–212
31. Weitzman SA, Stossel TP: Mutation caused by human phagocytes. Science 1981, 212:546–547
32. Weitberg AB, Weitzman SA, Destrempes M, Latt SA, Stossel TP: Stimulated human phagocytes produce cytogenetic changes in cultured mammalian cells. N Engl J Med 1983, 308:26–30
33. Weitzman SA, Weitberg AB, Clark EP, Stossel TP: Phagocytes as carcinogens: Malignant transformation produced by human neutrophils. Science 1985, 227:1231–1233
34. Cerutti PA: Prooxidant states and tumor promotion. Science 1985, 227:375–381
35. Davis JMG: An electron microscope study of the response of mesothelial cells to the intrapleural injection of asbestos dust. Br J Exp Pathol 1974, 55:64–70
36. Davis JMG: Histogenesis and fine structure of peritoneal tumors produced in animals by injections of asbestos. J Natl Cancer Inst 1974, 52:1812–1837
37. Timbrell V, Rendall REG: Preparation of the UICC standard reference sample of asbestos. Powder Technol 1971/72, 5:279–287
38. Brody AR, George G, Hill LH: Interactions of chrysotile and crocidolite asbestos with red blood cell membranes. Chrysotile binds to sialic acid. Lab Invest 1983, 49:468–475
39. Conrad RE: Induction and collection of peritoneal exudate macrophages, Manual of Macrophage Methodology: Collection, Characterization and Function. Edited by HB Herscowitz, HT Holden, JA Bellanti, A Ghaffar. New York, Marcel Dekker, 1981, pp 5–12
40. Macdonald JL, Kane AB: Identification of asbestos fibers within single cells. Lab Invest 1986, 55:177–185
41. Leak LV: Interaction of mesothelium to intraperitoneal stimulation: I. Aggregation of peritoneal cells. Lab Invest 1983, 48:479–491

42. Churg A, Warnock M: Asbestos fibers in the general population. Am Rev Respir Dis 1980, 122:669–678
43. Harrison CJ, Allen TD, Britch M, Harris R: High-resolution scanning electron microscopy of human metaphase chromosomes. J Cell Sci 1982, 56:409–422
44. Bjorkerud S, Bondjers G: Endothelial integrity and viability in the aorta of the normal rabbit and rat as evaluated with dye exclusion tests and interference contrast microscopy. Atherosclerosis 1972, 15:285–300
45. Lee RMKW, Chambers C, O'Brodovich H, Forrest JB: Trypan blue method for the identification of areas of damage to airway epithelium due to mechanical trauma. Scan Electron Microsc 1984, 111:1267–1271
46. Whitaker D, Papadimitriou JM, Walters MN-I: The mesothelium: Techniques for investigating the origin, nature and behavior of mesothelial cells. J Pathol 1980, 132:263–271
47. Williams MA: Autoradiography: Its methodology at the present time. J Microsc 1982, 128:79–94
48. Beck BD, Brain JD, Bohannon DE: An *in vivo* hamster bioassay to assess the toxicity of particulates for the lungs. Toxicol Appl Pharmacol 1982, 66:9–29
49. Doumas BT, Watson W, Biggs HG: Albumin standards and the measurement of serum albumin with bromcresol green. Clin Chim Acta 1971, 31:87–90
50. Cabaud PG, Wroblewski F: Colorimetric measurement of lactic dehydrogenase activity of body fluids. Am J Clin Pathol 1958, 30:234–236
51. Leak LV, Rahil K: Permeability of diaphragmatic mesothelium: The ultrastructural basis for "stomata." Am J Anat 1978, 151:557–594
52. Wang N-S: Mesothelial cells in situ, The Pleura in Health and Disease. Edited by J Chretien, J Bignon, A Hirsch. New York, Marcel Dekker, 1985, pp 23–42
53. Tsilibary E, Wissig SL: Absorption from the peritoneal cavity: SEM study of the mesothelium covering the peritoneal surface of the muscular portion of the diaphragm. Am J Anat 1977, 149:127–133
54. Roser BJ: The origin and significance of macrophages in thoracic duct lymph. Australian J Exp Biol Med Sci 1976, 54:541–550
55. Courtice FC, Harding J, Steinbeck AW: The removal of free red blood cells from the peritoneal cavity of animals. J Exp Biol Med Sci 1953, 31:215–225
56. Allen L, Weatherford T: Role of fenestrated basement membrane in lymphatic absorption from peritoneal cavity. Am J Physiol 1959, 197:551–554
57. Miller K, Kagan E: The in vivo effects of asbestos on macrophage membrane structure and population characteristics of macrophages: A scanning electron microscope study. J Reticuloendothel Soc 1976, 20:159–171
58. Whitaker D, Papadimitriou J: Mesothelial healing: Morphological and kinetic investigations. J Pathol 1985, 145:159–175
59. Corry D, Kulkarni P, Lipscomb MF: The migration of bronchoalveolar macrophages into hilar lymph nodes. Am J Pathol 1984, 115:321–328
60. Harmsen AG, Muggenburg BA, Snipes MB, Bice DE: The role of macrophages in particle translocation from lungs to lymph nodes. Science 1985, 230:1277–1280
61. Kagan E, Oghiso Y, Harmann D-P: Enhanced release of chemoattractant for alveolar macrophages after asbestos inhalation. Am Rev Respir Dis 1983, 128:680–687
62. Warheit DB, George G, Hill LH, Snyderman R, Brody AR: Inhaled asbestos activates a complement-dependent chemoattractant for macrophages. Lab Invest 1985, 52:505–514
63. Brody AR, Hill LH: Interstitial accumulation of inhaled chrysotile asbestos fibers and consequent formation of microcalcifications. Am J Pathol 1982, 109:107–114
64. Bowden DH, Adamson IYR: Bronchiolar and alveolar lesions in the pathogenesis of crocidolite-induced pulmonary fibrosis in mice. J Pathol 1985, 147:257–267
65. Hamilton JA: Macrophage stimulation and the inflammatory response to asbestos. Environ Health Persp 1980, 34:63–74
66. Werb Z: How the macrophage regulates its extracellular environment. Am J Anat 1983, 166:237–256
67. Whitaker D, Papadimitriou JM, Walters M N-I: The mesothelium and its reactions: A review. CRC Crit Rev Toxicol 1982, April:81–144
68. Raftery AT: Regeneration of the parietal and visceral peritoneum in the immature animal: A light and electron microscopical study. Br J Surg 1973, 60:969–975
69. Bolen JW, Hammar SP, McNutt MA: Reactive and neoplastic serosal tissue: A light-microscopic, ultrastructural and immunocytochemical study. Am J Surg Pathol 1986, 10:34–47
70. Winkler GC, Ruttner JR: Early fibrogenicity of asbestos fibers in visceral peritoneum. Exp Cell Biol 1983, 51:1–8
71. Hillerdal G: The pathogenesis of pleural plaques and pulmonary asbestosis: possibilities and impossibilities. Eur J Respir Dis 1980, 61:129–138
72. Herbert A: Pathogenesis of pleurisy, pleural fibrosis, and mesothelial proliferation. Thorax 1986, 41:176–189
73. Hamilton J, Vassalli JD, Reich E: Macrophage plasminogen activator: Induction by asbestos is blocked by anti-inflammatory steroids. J Exp Med 1976, 144:1689–1694
74. Whitaker D, Papadimitriou JM, Walters M N-I: The mesothelium: Its fibrinolytic properties. J Pathol 1982, 136:291–299

Acknowledgments

We gratefully acknowledge Robert Crausman and Linda Pietras for their technical assistance and Christine Levesque for preparation of the manuscript. An abstract of this work was presented at the annual meeting of the American Thoracic Society in 1986 and published in the *American Review of Respiratory Disease* (1986, 133:A198).